IEEE Open Journal of Signal Processing

Received 14 September 2023; revised 8 January 2024; accepted 16 January 2024. Date of publication 1 February 2024; date of current version 20 March 2024. The review of this article was arranged by Associate Editor Usman A Khan.

Digital Object Identifier 10.1109/OJSP.2024.3360860

A Family of Swish Diffusion Strategy Based Adaptive Algorithms for Distributed Active Noise Control

RAJAPANTULA KRANTHI [1] (Graduate Student Member, IEEE), VASUNDHARA [1] (Member, IEEE), ASUTOSH KAR [2] (Senior Member, IEEE), AND MADS GRÆSBØLL CHRISTENSEN [3] (Senior Member, IEEE)

[1]Department of Electronics and Communication Engineering, National Institute of Technology, Warangal, Telangana 506004, India
[2]Department of Electronics and Communication Engineering, Dr B R Ambedkar National Institute of Technology Jalandhar, Jalandhar 144008, India
[3]Department of Electronic Systems, Aalborg University, DK-9220 Aalborg, Denmark

CORRESPONDING AUTHOR: VASUNDHARA (email: vasundhara@nitw.ac.in).

This work was supported by the Ministry of Human Resource Development (MHRD), Government of India.

ABSTRACT The conventional filtered-x least mean square (F-xLMS) algorithm based distributed active noise control (DANC) system's performance suffers in the presence of outliers and impulse like disturbances. In an attempt to reduce noise in such an environment Swish function based algorithms for DANC systems have been proposed presently. The Swish function makes use of the smoothness and unboundedness properties for faster convergence and eliminating vanishing gradient issue. The intention is to employ the smooth approximation of Softplus and the non-convex property of Geman-McClure estimator to propose a Softplus Geman-McClure function. In addition, the bounded nonlinearity of Welsch function which is insensitive to the outliers is utilized with the regularization property of Softsign formulating Softsign Welsch method. Henceforth, this paper proposes a family of robust algorithms employing the Swish diffusion strategy for filtered-x sign, filtered-x LMS, filtered-x Softplus Geman-McClure and filtered-x Softsign Welsch algorithms for DANC systems. The weight update rules are derived for the proposed algorithms and convergence analysis is also carried out. The suggested methods achieve faster convergence in comparison with existing techniques and approximately 1–5 dB improvement in noise cancellation for various noise inputs and impulsive noise interferences.

INDEX TERMS Distributed active noise control, impulsive noise, robust adaptive filter, swish function.

I. INTRODUCTION

Wireless microphone networks, also known as wireless acoustic sensor networks (WASNs), are used in next-generation audio processing and acquisition technologies. Due to WASNs scalability and adaptability, the signal processing industry has recently become very interested in the topic of using WASNs to replace fixed multi-channel sound systems [1]. The WASNs perform distributed signal processing technique on the acoustic signals captured by the sensor nodes. However, various acoustic systems have been put forth, whose nodes are not only outfitted with microphones but may also control one or more loudspeakers or actuators [2]. These nodes also exhibit computational capability and information sharing with the adjacent nodes. The activities associated with sound field control includes active noise control (ANC), can all be carried out by this new class of WASNs [3]. Active noise control entails the notion of destructive interference. The basic structure of ANC comprises of reference, error microphone and a secondary path referring to amplifier loudspeaker combination. The filtered-x least mean square (F-xLMS) approach has been employed extensively in the Gaussian environment due to its low processing cost and compact design as an outstanding adaptive technique for ANC [4], [5], [6]. The well-known F-xLMS algorithm for broadband ANC is given a detailed statistical convergence analysis encompassing its performance in transient and steady-state situations [7]. Wave-domain adaptive methods for ANC are discussed in [8]. Multi-channel ANC (MANC) systems are widely used noise reduction strategies

that are computationally complex. Furthermore, noise mitigation for frequently heard disturbances is a challenging task, especially in multi-point situations [9], [10], [11]. The conventional approach of utilizing the centralised processing in a single and multi-channel systems are not scalable, necessitating the restructuring of update rules and the reorganisation of the hardware components. The centralized system faces the limitations of heavy computations, complexities and communication hindrance. In multichannel ANC system, weight update of each controller requires the errors corresponding to all channels, whereas distributed ANC updates the weight of each controller based on the error associated with precisely the same node. As a result, the MANC system incurs significant computing costs as it integrates all error signals. Additionally, the decentralised multichannel ANC system deals with computing complexity, however acoustical coupling problems arise between the loudspeakers of secondary paths and error microphones [12]. Two decentralized ANC systems were implemented in [13], [14].

Further, the distributed ANC setup reduces computational expenses by relying on an information sharing and the cooperation technique among neighbouring nodes. This enables the DANC system to function even if one or more paths of the central processor fails. Each DANC system node comprises of one error microphone, one secondary loudspeaker and a controller weight update module that allows for the adaption of the controller's own weights. This is accompanied by sharing information and cooperating with neighbouring nodes [15]. In a distributed method, the robustness of a system improves by amalgamating the controller parameters according to predetermined combination rules without significantly increasing computational cost. The development of diffusion [16] and incremental [17] learning strategies are the two common approaches for node cooperation to address this problem. Active noise cancellation encounter issues with impulse-like noises in error microphones and outliers in secondary channels because of faulty sensors, measurement errors, and microphone or loudspeaker movement. The presence of impulsive noise deteriorates the influence of the algorithms and computational cost increases. In lieu of this, various robust algorithms such as the sign algorithm (SA) [18], least mean forth (LMF) [19], maximum correntropy criterion (MCC) [20] and M-estimate [21], [22] are proposed for varied applications. Another robust functions such as variable step-size normalized LMS, techniques involving cosine functions such as exponential hyperbolic cosine function (EHCF), logarithmic hyperbolic cosine adaptive filter (LHCAF) are being utilized for different applications like system identification [23], ANC [24], diffusion channel estimation [25] respectively. Another approach involving information-theoretic learning strategy has been put forth utilizing maximum correntropy criterion (MCC) [26] and filtered-x generalized maximum correntropy criterion (F-xGMCC) for active noise control [27]. The improved filtered-x generalised maximum correntropy criterion (IF-xGMCC) method that uses continuous mixed Lp-norm overcomes the slow convergence rate and less noise reduction performance of (F-xGMCC) technique [28]. An effective ANC using Wilcoxon filtered-x least mean square (WF-xLMS) algorithm which is resistant to outliers in the secondary pathways and burst noise recorded by a defective microphone has been suggested in [29]. Lately, a generalized modified Blake–Zisserman (GMBZ) technique is initiated for system identification to offer robustness against non-Gaussian/impulsive noise without compromising steady-state misalignment is presented in [30]. The nodes of an acoustic sensor network using a distributed affine projection (AP) method are acoustically connected and presented in [31]. Recently, robust techniques pertaining to maintaining the performance of active noise control in the wake of impulsive noise interference have been introduced such as: error reused filtered-x LMS (ErF-xLMS) [32], modified filtered-x robust normalized least mean absolute third (MF-xRNLMAT) [33] and modified filtered-x affine-projection-like MCC (MFxAPLMCC) [34]. In addition, a combination of regularization factors by virtue of a mixing parameter for affine projection algorithm is discussed in [35]. A robust arctangent framework is presented for system identification in [36].

A robust distributed active noise control system (RDANC) to combat the impulsive noise using R-estimator is developed in [37]. A distributed filtered-x least mean square (F-xLMS) approach for a DANC system and its efficacy is assessed in [38], [39], [40]. One of the major issues in the impulsive environment for adaptive filtering is choosing a suitable cost function for DANC. Many methods have been designed by incorporating the standard cost functions into the sigmoid framework and taking advantage of the sigmoid's saturation property [41]. Whatever the input, the sigmoid function suffers from the vanishing gradient problem if their value saturates. It is a logistic function with an output in the range [0, 1]. Due to this nature the sigmoid function takes longer time to converge. For $x < 0$ the gradient fail to flow backwards. The above two drawbacks motivate towards Swish function. The suggested Swish function integrated with diffusion strategy as Swish diffusion (SD) based algorithms for the DANC system are designed with a purpose of maintaining system performance in varied impulsive noise situations. The combined nature of Softplus smooth approximation and non convexity of Geman-McClure leads to Softplus Geman-McClure (SGM) function. The Welsch bounded nonlinear property with Softsign smoothing is insensitive to impulsive noise which can eliminate large outliers and make the system stable, leads to formulate Softsign Welsch (SW) function. To enhance the performance of the DANC systems SGM and SW are incorporated into the Swish function. The Swish diffusion filtered-x sign algorithm (SDF-xSA), Swish diffusion filtered-x LMS (SDF-xLMS), Swish diffusion filtered-x Softplus Geman-McClure (SDF-xSGM) and Swish diffusion filtered-x Softsign Welsch (SDF-xSW) are the various robust algorithms that are proposed using the framework of Swish diffusion strategy. In this research, we derive the coefficients adaptation rule for the proposed SD algorithms in diffusion frame for a distributed ANC environment. Numerous

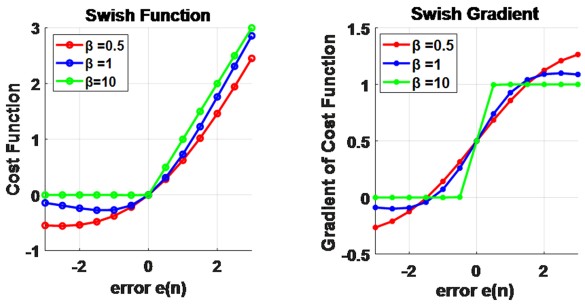

FIGURE 1. Swish function and its gradient for different beta values.

simulations have been conducted in the DANC scenario to examine the performance of the aforementioned techniques for varied input reference noises. The key attributes of this paper are listed as:

1) The paper attempts to formulate a family of distributed ANC systems utilising a diffusion technique integrated with the Swish function while maintaining performance of the system across various impulsive noise environment.
2) The smoothness imparted by Softplus and the inherent non convex property of Geman-McClure is combined to introduce a robust Softplus Geman-McClure (SGM) function.
3) The smoothness of Softsign and bounded nonlinear property of Welsch leads to the development of Softsign Welsch(SW) function.
4) In lieu of this, Swish diffusion function (SD) based distributed ANC framework is developed for a family of algorithms such as Swish diffusion filtered-x sign algorithm (SDF-xSA), Swish diffusion filtered-x LMS (SDF-xLMS), Swish diffusion filtered-x Softplus Geman-McClure (SDF-xSGM) and Swish diffusion filtered-x Softsign Welsch (SDF-xSW) in a distributed ANC environment.
5) The weight update rule for a class of suggested Swish diffusion algorithms are obtained in this paper. The stability analysis is done for the suggested technique in terms of the mean convergence.

II. PRELIMINARIES

Swish function is proposed which is given as

$$f(x) = x \cdot \frac{1}{1 + e^{-\beta x}} \tag{1}$$

According to (1), this function is unbounded for $x > 0$, preventing saturation, it does not become zero for $x < 0$, allowing gradient to flow and preventing vanishing gradient problem. In (1), β is a positive control parameter which controls the steepness of the Swish function [42] and Fig. 1 represents Swish function with their corresponding gradients for different β values respectively. If $\beta = 0$, the Swish function is linear in nature. As $\beta \to \infty$ the sigmoid term approaches a 0-1 function, which makes Swish as a rectified linear unit. It has been viewed from literature review that a very few amount of research work is accomplished for developing robust DANC schemes. Therefore, it is necessitated to maintain the performance of the DANC system under impulsive noise environment. In lieu of this to combat the large impulsive noise, an attempt has been made in this study to construct a robust DANC system using Swish as the cost function.

The rest of the manuscript is structured as: In Section III, the suggested robust Swish based cost functions are formulated. Further, the weight adaption rules are derived for the introduced family of robust DANC techniques. Section IV, discusses the convergence analysis of Swish diffusion DANC approach.The simulation and discussions are used to validate the suggested strategy in Section V. Section VI deals with conclusions.

III. PROPOSED ROBUST SWISH DIFFUSION DANC SCHEMES

In this manuscript an attempt has been made to actively control noise via an adaptive process using diffusion strategy considering in total K number of nodes. Each node shares information with other remaining nodes in the DANC system. In distributed active noise set-up, each node signifies an ANC module consisting of a reference microphone, a loudspeaker and an error sensor. Consider a distributed active noise control application with input as reference noise $\mathbf{x}(n)$. Fig. 2 shows the block diagram of DANC module, where K number of nodes are displayed. The internal module and functionality of k^{th} node which in turn represents an ANC module is further expanded in Fig. 2. In Fig. 2, node 1 is considered as the central node entrusted with the task of generating diffused weight vector from the updated weight vectors received from all the other nodes of the distributed set-up.

In the current manuscript, a distributed network comprising of $1 \times J \times K$ structure is presented. In this regard, K signifies the total number of error microphones whereas J represents the total numbers of secondary loudspeakers. Furthermore, the number of error microphones K is considered equivalent to secondary sources J and $J = K = 5$. The internal structure of each node includes a primary path, secondary path and controller weight update module. The input reference signal detected by the reference input microphone travels along the primary path and leads to the primary noise. The controller output is superimposed on the primary path after passing through the secondary path at quiet zone. Error sensor at k^{th} node determines the residual error $e_k(n)$ between the primary pathways output $d_k(n)$ and secondary pathways output $y_k(n)$. The output impulsive noise $v_k(n)$ added to the model is obtained by SαS model as shown in Fig. 2. The unboundedness and the smoothness of the Swish function inspires to build a frame work of Swish diffusion DANC.

The proposed Swish cost function (SCF) is formulated as

$$\text{SCF} = \xi_k(n)\text{sgm}[\beta\xi_k(n)] \tag{2}$$

where sgm represents sigmoid and $\xi_k(n)$ is the error cost function incorporated in (2) to develop the Swish based four

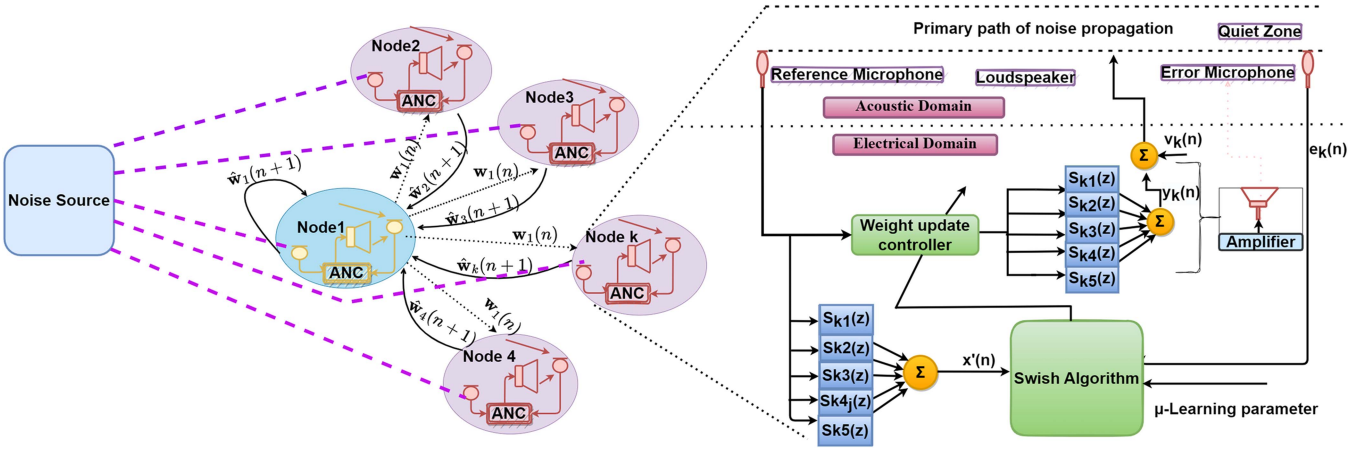

FIGURE 2. Block diagram of Swish diffusion DANC.

algorithms such as SDF-xSA, SDF-xLMS, SDF-xSGM and SDF-xSW. The output generated by the controller at k^{th} node is obtained as

$$\tilde{y}_k(n) = \mathbf{x}(n)^{\mathrm{T}}\mathbf{w}_k(n), \tag{3}$$

where $\mathbf{x}(n) = [x(n), x(n-1), x(n-2), \ldots, x(n-L+1)]^{\mathrm{T}}$ is the reference input given to the microphone, T represents the transpose operator and L is the length of the weight vector of the controller.

$\hat{\mathbf{w}}_k(n) = [\hat{\mathbf{w}}_k^0(n), \hat{\mathbf{w}}_k^1(n), \ldots, \hat{\mathbf{w}}_k^{L-1}(n)]^{\mathrm{T}}$ is the controller weight update at the k^{th} node. $\mathbf{w}_k(n)$ is the diffused weight vector at k^{th} node obtained as

$$\mathbf{w}_k(n) = \sum_{m\in K} A_{km}\hat{\mathbf{w}}_m(n). \tag{4}$$

A_{km} is a pre-selected value such that $\sum_{m\in K} A_{km} = 1$ [16] to obtain the average weight vector $\mathbf{w}_k(n)$ by using the local estimates i.e. $\hat{\mathbf{w}}_m(n)$, which are fused at k^{th} node over the neighbourhoods $m \in K$ [12]. The estimation error at k^{th} node is evaluated as given below

$$\begin{aligned} e_k(n) &= d_k(n) - y_k(n), \\ &= d_k(n) - \sum_{j=1}^{J} \mathbf{S}_{kj}(n) * \tilde{y}_k(n), \\ &= d_k(n) - \sum_{j=1}^{J} \mathbf{S}_{kj}(n) * \left[\mathbf{x}(n)^{\mathrm{T}}\mathbf{w}_k(n)\right]. \end{aligned} \tag{5}$$

where $d_k(n)$ is the output of the primary path and $y_k(n) = \sum_{j=1}^{J} \mathbf{S}_{kj}(n) * [\mathbf{x}(n)^{\mathrm{T}}\mathbf{w}_k(n)]$ representing the final filtered output at k^{th} node while accounting all the secondary path coupling effects and $*$ shows convolution operator. This is modelled in terms of $\mathbf{S}_{kj}(n)$ representing coupling between k^{th} error sensor to the j^{th} loudspeaker of other node. In (5), J denotes the total number of loudspeakers. In the present work we have considered $J = K = 5$ for simplification purpose. The cost function utilized to calculate the update weight vectors for the controller coefficients at the k^{th} node is defined as follows: $\mathrm{SCF} = \xi_k(n)\mathrm{sgm}[\beta\xi_k(n)]$. The weight update for the active noise controller taps is achieved using the stochastic gradient method as

$$\begin{aligned} \hat{\mathbf{w}}_k(n+1) &= \mathbf{w}_k(n) - \mu\frac{\partial \mathrm{SCF}}{\partial \mathbf{w}_k(n)}, \\ \hat{\mathbf{w}}_k(n+1) &= \mathbf{w}_k(n) \\ &\quad + \mu\left\{\frac{1+[1-\beta\xi_k(n)]\exp(-\beta\xi_k(n))}{[1+\exp(-\beta\xi_k(n))]^2}\right\}\left\{\frac{\partial\xi_k(n)}{\partial\mathbf{w}_k(n)}\right\}, \end{aligned} \tag{6}$$

where,

$$\frac{\partial \mathrm{SCF}}{\partial \mathbf{w}_k(n)} = \left\{\frac{1+[1-\beta\xi_k(n)]\exp(-\beta\xi_k(n))}{[1+\exp(-\beta\xi_k(n))]^2}\right\}\left\{\frac{\partial\xi_k(n)}{\partial\mathbf{w}_k(n)}\right\}, \tag{7}$$

where $\xi_k(n)$ will vary according to the development of SDF-xSA, SDF-xLMS, SDF-xSGM and SDF-xSW. $\hat{\mathbf{w}}_k(n+1)$ is the adaptive controller weight update coefficient vector at $(n+1)^{th}$ iteration of k^{th} node and μ represents the convergence factor.

A. DERIVATION FOR SWISH DIFFUSION FILTERED-X SIGN ALGORITHM (SDF-XSA)

Substituting the error cost function as $\xi_{k1}(n) = E[|e_k(n)|]$, inspired by sign algorithm [18] into the Swish cost function as defined in (2) and using the same as $\mathrm{SCF}_1 = \xi_{k1}(n)\mathrm{sgm}[\beta\xi_{k1}(n)]$. The weight update of the proposed Swish diffusion filtered-x sign algorithm (SDF-xSA), is obtained as

$$\begin{aligned} \hat{\mathbf{w}}_k(n+1) &= \mathbf{w}_k - \mu\frac{\partial \mathrm{SCF}_1}{\partial \mathbf{w}_k(n)}, \\ \hat{\mathbf{w}}_k(n+1) &= \mathbf{w}_k(n) + \mu\mathrm{sign}(e_k(n)) \\ &\quad \times \frac{\left[1+\{1-\beta|e_k(n)|\}\exp\left(-\beta|e_k(n)|\right)\right]}{\left[1+\exp\left(-\beta|e_k(n)|\right)\right]^2}\mathbf{x}'(n), \end{aligned} \tag{8}$$

where $\mathbf{x}'(n) = \sum_{j=1}^{J} \mathbf{S}_{kj}(n) * \mathbf{x}(n)^{\mathrm{T}}$ is the filtered input signal. $\mathbf{S}_{kj}$ signifies secondary pathways between the k^{th} error

microphone and the j^{th} loudspeaker path and

$$\frac{\partial e_k(n)}{\partial \mathbf{w}_k(n)} = -\sum_{j=1}^{J} \mathbf{S}_{kj}(n) * \mathbf{x}(n)^{\mathrm{T}}. \tag{9}$$

B. DERIVATION FOR SWISH DIFFUSION FILTERED-X LEAST MEAN SQUARE ALGORITHM (SDF-XLMS)

The cost function of the mean square error (MSE) based traditional LMS [4] method is $\xi_{k2}(n) = E[e_k^2(n)]$. The weight update of the suggested SDF-xLMS method is obtained by minimizing the cost function $\mathrm{SCF}_2 = \xi_{k2}(n)\mathrm{sgm}[\beta\xi_{k2}(n)]$ and employing $\xi_{k2}(n) = E[e_k^2(n)]$ using stochastic gradient approach as

$$\hat{\mathbf{w}}_k(n+1) = \mathbf{w}_k(n) - \mu\frac{\partial \mathrm{SCF}_2}{\partial \mathbf{w}_k(n)},$$

$$\hat{\mathbf{w}}_k(n+1) = \mathbf{w}_k(n) + \mu 2e_k(n) \times \frac{\left[1 + \left\{1 - \beta e_k^2(n)\right\}\exp\left(-\beta e_k^2(n)\right)\right]}{\left[1 + \exp\left(-\beta e_k^2(n)\right)\right]^2}\mathbf{x}'(n). \tag{10}$$

where $\mathbf{x}'(n) = \sum_{j=1}^{J} \mathbf{S}_{kj}(n) * \mathbf{x}(n)^{\mathrm{T}}$.

C. DERIVATION FOR SWISH DIFFUSION FILTERED-X SOFTPLUS GEMAN-MCCLURE ALGORITHM (SDF-XSGM)

The smooth non-convex nature of Softplus Geman-McClure estimator compresses the data with large amplitude for effectively optimizing the error criterion while training DANC systems. The Geman-McClure with Softplus is defined in this paper as $\chi = \ln(1 + \exp(\epsilon))$ where $\epsilon = \frac{e_k(n)^2}{e_k(n)^2 + c_1^2}$ and c_1 is the shaping parameter of SGM. The suggested cost function of the SDF-xSGM algorithm is obtained by substituting $\xi_{k3}(n) = E[\ln(1 + \exp(\epsilon))]$ in the Swish cost function defined $\mathrm{SCF}_3 = \xi_{k3}(n)\mathrm{sgm}[\beta\xi_{k3}(n)]$. Further, the controller weight update of the proposed SDF-xSGM is obtained as

$$\hat{\mathbf{w}}_k(n+1) = \mathbf{w}_k(n) - \mu\frac{\partial \mathrm{SCF}_3}{\partial \mathbf{w}_k(n)},$$

$$\hat{\mathbf{w}}_k(n+1) = \mathbf{w}_k(n) + \mu \times \frac{2e_k(n)c_1^2\left[1 + \left(\exp(-\beta\phi)(1 - \beta\phi)\right]\mathbf{x}'(n)\right.}{\left(e_k^2(n)+c_1^2\right)^2\left[1+\exp\left(\frac{e_k^2(n)}{e_k^2(n)+c_1^2}\right)(1+exp(-\beta\phi))\right]}. \tag{11}$$

where $\mathbf{x}'(n) = \sum_{j=1}^{J} \mathbf{S}_{kj}(n) * \mathbf{x}(n)^{\mathrm{T}}$ and

$$\phi = \ln\left(1 + \exp\left(\frac{e_k^2(n)}{e_k^2(n) + c_1^2}\right)\right).$$

D. DERIVATION FOR SWISH DIFFUSION FILTERED-X SOFTSIGN WELSCH ALGORITHM (SDF-XSW)

The Welsch bounded nonlinear property with Softsign smoothing is insensitive to impulsive noise which can eliminate large outliers and make the system stable. This leads to the development of Softsign Welsch (SW) function as $\Phi = \exp\{-(\Theta/c_2)^2\}$, $\Theta = \frac{e_k(n)}{1+|e_k(n)|}$ and c_2 is the shaping parameter. The weight update of the SDF-xSW method is obtained by substituting $\xi_{k4}(n) = E[\exp\{-(\Theta/c_2)^2\}]$ into the proposed Swish cost function $\mathrm{SCF}_4 = \xi_{k4}(n)\mathrm{sgm}[\beta\xi_{k4}(n)]$ as $\hat{\mathbf{w}}_k(n+1) = \mathbf{w}_k(n) - \mu\frac{\partial \mathrm{SCF}_4}{\partial \mathbf{w}_k(n)}$,

$$\hat{\mathbf{w}}_k(n+1) = \mathbf{w}_k(n) + \mu \frac{2e_k(n)(|e_k(n)| - 1)\delta}{c_2^2(1 + |e_k(n)|)^3}\left[\frac{1 + \exp(-\beta\delta)\{1 - \beta\delta\}}{\{1 + \exp(-\beta\delta)\}^2}\right]\mathbf{x}'(n). \tag{12}$$

where $\mathbf{x}'(n) = \sum_{j=1}^{J} \mathbf{S}_{kj}(n) * \mathbf{x}(n)^{\mathrm{T}}$ and $\delta = \exp\left(-\left(\frac{e_k(n)}{(1+|e_k(n)|)c_2}\right)^2\right)$.

The variation of the SD-based cost function for the family of algorithms (SDF-xSA, SDF-xLMS, SDF-xSGM, SDF-xSW) along with it's derivative over the conventional one is shown in Fig. 3 for $\beta = 1$. Fig. 3 depicts that the Swish diffusion framework based cost function steepens with impulsive interference. Additionally, the gradient of the Swish diffusion framework based cost function is more constrained than conventional cost functions for large errors, providing robust performance. The comparison of the cost functions with respect to some robust functions for instance least mean square (LMS), robust normalized least mean absolute third (RNLMAT), generalized maximum correntropy criterion (GMCC), Blake Zisserman (BZ) are displayed in Fig. 4. It is indicated from Fig. 4 that the proposed SDF-xSGM reveal the characteristics of a robust cost function as compared to other techniques. Algorithm 1 represents the pseudo code of the proposed SD class of algorithms. Table 1 summarizes the proposed Swish based class of algorithms, cost functions and the corresponding weight update equations. The proposed DANC class of algorithms such as SDF-xSA, SDF-xLMS, SDF-xSGM, and SDF-xSW are compared with filtered-x sign algorithm (F-xSA), filtered-x LMS (F-xLMS), filtered-x Geman-McClure (F-xGM), filtered-x Welsch (F-xW) as shown in the Table 2 in terms of computations that are exhausted in multiplication, addition, division, exponential, absolute and sign operations. The following phases involved in the analysis of the suggested techniques are used to compute the total computational load: (1) output of the controller, (2) filtered version of the input signal and (3) weight update of the controller.

IV. BOUND FOR CONVERGENCE

The effectiveness of the SD algorithm is analysed for each of the nodes utilizing the system global data, which is specified as

$$\mathbf{d}(n) = \mathbf{X}(n)\mathbf{p} + \mathbf{v}(n). \tag{13}$$

To conduct an analytical study of the algorithm's performance in a wider perspective, we have used the global data concept where matrices and vectors are created by taking into account the information at each node. Therefore utilizing the global data notion for (13) we define, $\mathbf{d}(n) = \mathrm{col}\{d_1(n), \ldots, d_K(n)\}$

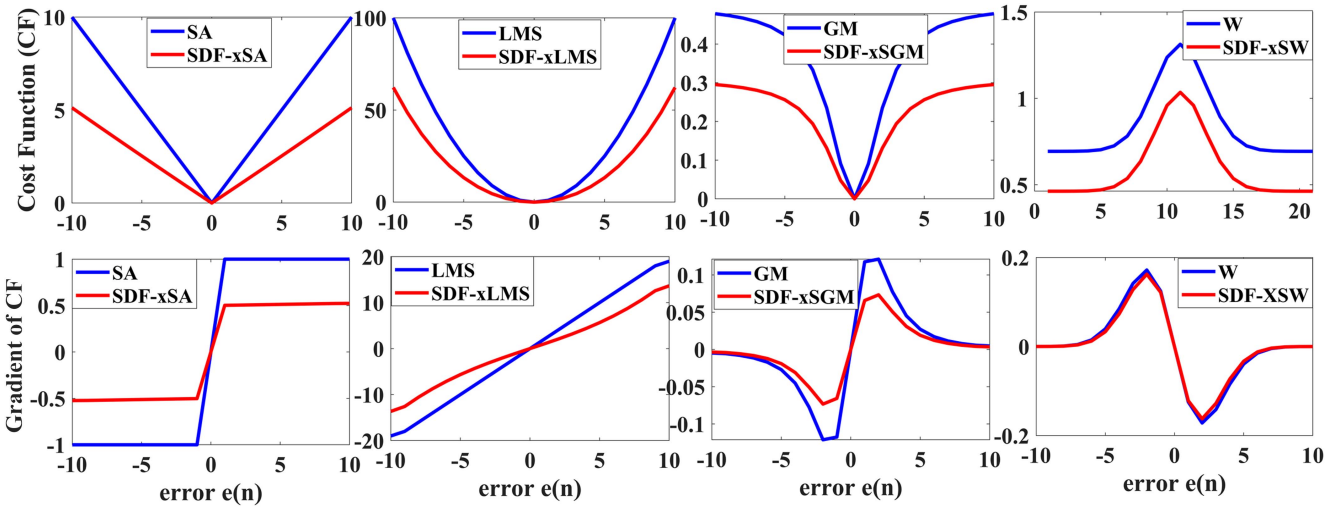

FIGURE 3. Comparison of the Swish cost function (SDF-xSA, SDF-xLMS, SDF-xSGM, SDF-xSW) along with its gradient.

TABLE 1. Proposed Swish Based Class of Algorithms and their Cost Functions

Swish framework	Error Cost function	Swish cost function(SCF)	Weight update equation for Swish function based algorithm
SDF-xSA	$\xi_{k1}(n) = E[\lvert e_k(n)\rvert]$	$\mathbf{SCF}_1 = \xi_{k1}(n)\mathrm{sgm}[\beta\xi_{k1}(n)]$	$\hat{\mathbf{w}}_k(n+1) = \mathbf{w}_k(n) + \mu\frac{[1+\{1-\beta\lvert e_k(n)\rvert\}\exp(-\beta\lvert e_k(n)\rvert)]}{[1+\exp(-\beta\lvert e_k(n)\rvert)]^2}\mathbf{x}'(n)$,
SDF-xLMS	$\xi_{k2}(n) = E[e_k^2(n)]$	$\mathbf{SCF}_2 = \xi_{k2}(n)\mathrm{sgm}[\beta\xi_{k2}(n)]$	$\hat{\mathbf{w}}_k(n+1) = \mathbf{w}_k(n) + \mu\frac{\left[1+\left\{1-\beta e_k^2(n)\right\}\exp\left(-\beta e_k^2(n)\right)\right]}{\left[1+\exp\left(-\beta e_k^2(n)\right)\right]^2}\mathbf{x}'(n)$
SDF-xSGM	$\xi_{k3}(n) = E[\ln(1+\exp(\epsilon))]$, $\epsilon = \frac{e_k(n)^2}{e_k(n)^2+c_1^2}$	$\mathbf{SCF}_3 = \xi_{k3}(n)\mathrm{sgm}[\beta\xi_{k3}(n)]$	$\hat{\mathbf{w}}_k(n+1) = \mathbf{w}_k(n) + \mu\frac{2e_k(n)c_1^2[1+(\exp(-\beta\phi)(1-\beta\phi)]}{\left(e_k^2(n)+c_1^2\right)^2\left[1+\exp\left(\frac{e_k^2(n)}{e_k^2(n)+c_1^2}\right)(1+exp(-\beta\phi))\right]}\mathbf{x}'(n)$, $\phi = \ln\left(1+\exp\left(\frac{e_k^2(n)}{e_k^2(n)+c_1^2}\right)\right)$
SDF-xSW	$\xi_{k4}(n) = E[\exp\{-(\Theta/c_2)^2\}]$, $\Theta = \frac{e_k(n)}{1+\lvert e_k(n)\rvert}$	$\mathbf{SCF}_4 = \xi_{k4}(n)\mathrm{sgm}[\beta\xi_{k4}(n)]$	$\hat{\mathbf{w}}_k(n+1) = \mathbf{w}_k(n) + \mu\frac{2e_k(n)(\lvert e_k(n)\rvert-1)\delta}{c_2^2(1+\lvert e_k(n)\rvert)^3}\left[\frac{1+\exp(-\beta\delta)\{1-\beta\delta\}}{\{1+\exp(-\beta\delta)\}^2}\right]\mathbf{x}'(n)$, $\delta = \exp\left(-\left(\frac{e_k(n)}{(1+\lvert e_k(n)\rvert)c_2}\right)^2\right)$

$\mathbf{x}'(n) = \sum_{j=1}^{J}\mathbf{S}_{kj}(n) * \mathbf{x}(n)^{\mathrm{T}}$, ϕ= proposed SGM cost function, δ= proposed SW cost function, ϵ is the Geman Mc- Clure function, Θ is the Welsch function, c_1=2 and c_2=1 are the shaping parameters of SGM and SW functions respectively.

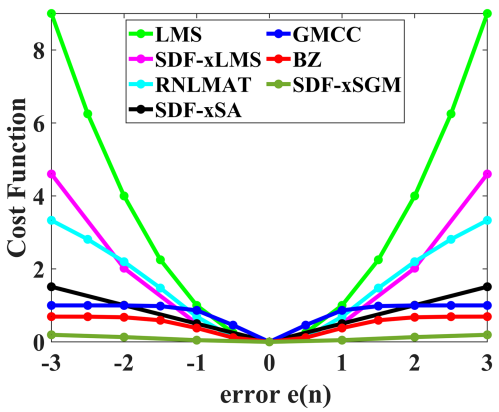

FIGURE 4. Comparison of the robust cost functions.

shows the desired output of size $(K \times 1)$, $\mathbf{X}(n) = \mathrm{diag}\{\mathbf{x}_1(n)^{\mathrm{T}}, \ldots, \mathbf{x}_k(n)^{\mathrm{T}} \ldots, \mathbf{x}_K(n)^{\mathrm{T}}\}$ is the input reference of size $(K \times KL)$, $\mathbf{p} = \mathrm{col}\{\boldsymbol{p}_1, \ldots, \boldsymbol{p}_k \ldots, \boldsymbol{p}_K\}$ is the primary path of size $(KL \times 1)$ and $\mathbf{v}(n) = \mathrm{col}\{\mathbf{v}_1(n), \ldots, \mathbf{v}_K(n)\}$ shows the impulsive noise added of size $(K \times 1)$. The controller weight update rule for the suggested DANC algorithm is specified as

$$\hat{\mathbf{w}}_k(n+1) = \mathbf{w}_k(n) + \mu\Upsilon_k(n)e_k(n)\mathbf{x}'_k(n), \tag{14}$$

where $\Upsilon_k(n)$ is robust error weighted parameter of Swish function described as

$$\Upsilon_k(n) = \left[\frac{1+[1-\beta\xi_k(n)]\exp(-\beta\xi_k(n))}{[1+\exp(-\beta\xi_k(n))]^2}\right].$$

The global data for (14) are defined as $\hat{\mathbf{w}}(n+1) = \mathrm{col}\{\hat{\mathbf{w}}_1(n+1), \ldots, \hat{\mathbf{w}}_K(n+1)\}$ is weight update controller of size $(KL \times 1)$, $\mathbf{w}(n) = \mathrm{col}\{\mathbf{w}_1(n), \ldots, \mathbf{w}_K(n)\}$ is average weight coefficients of size $(KL \times 1)$, $\Upsilon(n) = \mathrm{diag}\{\Upsilon_1(n), \ldots, \Upsilon_K(n)\}$ is the robust error weighted parameter of size $(K \times K)$, $\mathbf{B} = \mathrm{diag}\{\mu_1\mathbf{I}_L, \ldots, \mu_K\mathbf{I}_L\}$ is the learning rate parameter of size $(KL \times KL)$, $\mathbf{e}(n) = \mathrm{col}\{e_1(n), \ldots, e_K(n)\}$ is the residual noise error of size $(K \times 1)$ and $\mathbf{X}'(n) = \mathrm{diag}\{\mathbf{x}'_1(n)^{\mathrm{T}}, \ldots, \mathbf{x}'_K(n)^{\mathrm{T}}\}$ is the filtered input reference which is of size $(K \times KL)$. The weight update equation using the global data can be re-framed as

$$\hat{\mathbf{w}}(n+1) = \mathbf{w}(n) + \mathbf{B}\mathbf{X}'(n)^{\mathrm{T}}\Upsilon(n)\mathbf{e}(n), \tag{15}$$

TABLE 2. Comparison of Computational Complexity of SDF-xSA, SDF-xLMS, SDF-xSGM, SDF-xSW With F-xSA, F-xLMS, F-xGM, F-xW Method DANC Systems

Equation	Operation	Methods							
		F-xSA	SDF-xSA	F-xLMS	SDF-xLMS	F-xGM	SDF-xSGM	F-xW	SDF-xSW
Controller Output	MUL	LK	LK	LK	LK	LK	LK	LK	LK
	ADD	K(L-1)	K(L-1)	K(L-1)	K(L-1)	K(L-1)	K(L-1)	K(L-1)	K(L-1)
Filtered Signal	MUL	KJLs	KJLs	KJLs	KJLs	KJLs	KJLs	KJLs	KJLs
	ADD	KJ(Ls-1)	KJ(Ls-1)	KJ(Ls-1)	KJ(Ls-1)	KJ(Ls-1)	KJ(Ls-1)	KJ(Ls-1)	KJ(Ls-1)
Weight Update	MUL	KJLs+KL	KJLs+2KL+K	KJLs+KL	KJLs+KL+11K	KJLs+KL+9K	KJLs+KL+16K	KJLs+KL+7K	KJLs+KL+19K
	ADD	KJ(Ls-1)+KL-K	KJ(Ls-1)+4K(L-1)	KJ(Ls-1)+KL-K	KJ(Ls-1)+KL+5K	KJ(Ls-1)+KL+K	KJ(Ls-1)+KL+6K	KJ(Ls-1)+KL+4K	KJ(Ls-1)+KL+17K
	DIV	-	K	-	K	K	-	-	-
	EXP	-	2K	-	4K	-	5K	-	7K
	SIGN	K	K	-	-	-	-	-	-
	ABS	-	-	-	-	-	-	6K	8K
Total	MUL	2K(JLs+L)	K(2JLs+3L+1)	2K(JLs+L)	K(2JLs+2L+11)	K(2JLs+2L+9)	2K(JLs+L+8)	K(2JLs+2L+7)	K(2JLs+2L+19)
	ADD	2KJ(Ls-1)+2K(L-1)	2KJ(Ls-1)+5K(L-1))	2KJ(Ls-1)+2KL-2K	2KJ(Ls-1)+2KL+4K	2KJ(Ls-1)+2KL	2KJ(Ls-1)+2KL+5K	2KJ(Ls-1)+2KL+3K)	2KJ(Ls-1)+2KL+16K
	DIV	-	K	-	K	K	-	-	-
	EXP	-	2K	-	4K	-	5K	-	7K
	SIGN	K	K	-	-	-	-	-	-
	ABS	-	-	-	-	-	-	6K	8K

K = no. of error sensors, L = length of the controller, J = no. of loudspeakers, L_s = length of the secondary path coefficients, MUL = Multiplication, ABS = Absolute, ADD = Addition, EXP = Exponential, DIV = Division.

We redefined the proposed SD algorithm by substituting $\mathbf{w}(n) = \mathbf{G}\hat{\mathbf{w}}(n)$ in (15) as

$$\hat{\mathbf{w}}(n+1) = \mathbf{G}\hat{\mathbf{w}}(n) + \mathbf{B}\mathbf{X}'(n)^{\mathrm{T}}\Upsilon(n)\mathbf{e}(n), \tag{16}$$

where $\mathbf{G} = \mathbf{A} \otimes \mathbf{I}_L$ is the transition matrix $(KL \times KL)$, $\mathbf{A}$ is the metropolis matrix $(K \times K)$ with its coefficient A_{km} defined in (4) and $\otimes$ the Kronecker product. The global error expressed as $\mathbf{e}(n) = \mathbf{d}(n) - \mathbf{X}(n)\mathbf{S}\mathbf{G}\hat{\mathbf{w}}(n)$, where $\mathbf{S}$ is secondary pathways of size $(KL \times KL)$.

The mean analysis of the suggested SD approach is provided below: The robust error weighted parametric $\Upsilon(n)$, which is assumed to be independent of filtered input $\mathbf{X}'(n)$, establishes The maximal step size accepted for mean sense convergence. The global error coefficient weight vector is defined as $\widetilde{\mathbf{w}}(n) = \mathbf{w} - \hat{\mathbf{w}}(n)$. From the system model, the weight update equation of the controller is redefined as

$$\hat{\mathbf{w}}(n+1) = \mathbf{G} \cdot \hat{\mathbf{w}}(n) + \mathbf{B}\mathbf{X}'(n)^{\mathrm{T}}\Upsilon(n) \times \{\mathbf{d}(n) - \mathbf{X}(n)\mathbf{S}\mathbf{G}\hat{\mathbf{w}}(n)\}. \tag{17}$$

since $\mathbf{G}\mathbf{w} = \mathbf{w}$, subtract the right hand side of (17) from $\mathbf{G}\mathbf{w}$ and the left hand side from $\mathbf{w}$ and using $\widetilde{\mathbf{w}}(n) = \mathbf{w} - \hat{\mathbf{w}}(n)$, the expectation of the global weighted coefficient error vector is obtained as

$$E[\widetilde{\mathbf{w}}(n+1)] = \mathbf{G}E[\widetilde{\mathbf{w}}(n)] - E\left[\mathbf{B}\mathbf{X}'(n)^{\mathrm{T}}\Upsilon(n)\mathbf{X}(n)\mathbf{S}\mathbf{G}\widetilde{\mathbf{w}}(n)\right], \tag{18}$$

where $E[.]$ is the expectation operator.

$$E[\widetilde{\mathbf{w}}(n+1)] = [\mathbf{I}_{KL} - \mathbf{B}E[\mathbf{X}'(n)^{\mathrm{T}}\Upsilon(n)\mathbf{X}'(n)]]\mathbf{G}E[\widetilde{\mathbf{w}}(n)], \tag{19}$$

In the compact form,

$$E[\mathbf{X}'(n)^{\mathrm{T}}\Upsilon(n)\mathbf{X}'(n)] = \mathbf{R}_X\mathbf{R}_\Upsilon, \tag{20}$$

where $\mathbf{R}_X = E[\mathbf{X}'(n)^{\mathrm{T}}\mathbf{X}'(n)]$ is the auto-correlation matrix and $\mathbf{R}_\Upsilon = E[\Upsilon(n)] \bigotimes \mathbf{I}_L$. Using (19) and (20), we get

$$E[\widetilde{\mathbf{w}}(n+1)] = \mathbf{D}\mathbf{G}E[\widetilde{\mathbf{w}}(n)], \tag{21}$$

where $\mathbf{D} = [\mathbf{I}_{KL} - \mathbf{B}\mathbf{R}_X\mathbf{R}_\Upsilon]$. The greatest eigenvalue of the matrix $\mathbf{D}\mathbf{G}$ should be less than one so as to make the technique stable in the mean sense i.e. $|\lambda_{\max}(\mathbf{D}\mathbf{G}) < 1|$. As the cooperative technique improves the stability situation, therefore $|\lambda_{\max}(\mathbf{D}\mathbf{G})| < |\lambda_{\max}(\mathbf{D})|$. Therefore $|\lambda_{\max}(\mathbf{D})| < 1$, is enough to prove the condition's stability in the mean sense. This condition holds if the step size μ_k adheres to the constraints given below

$$0 < \mu_k < \frac{2}{\lambda_{\max}\left(\mathbf{R}_{X,k}\right) E\left[\Upsilon_k(n)\right]}.$$

where $\mathbf{R}_{X,k} = E[\mathbf{X'}_k(n)^{\mathrm{T}}\mathbf{X'}_k(n)]$.

V. RESULTS AND DISCUSSIONS

The robustness of the suggested algorithms are evaluated for various scenarios in this section. The input references used for the simulations are case (A): uniformly distributed noise, case (B): chaotic noise, case (C): three real noises such as factory noise, airplane cabin noise and traffic noise, case (D): comparative analysis of the proposed algorithms and case (E) real-world scenario. The input reference signal is uniformly distributed between −0.5 and 0.5. The chaotic

Algorithm 1: Pseudocode for the Suggested Algorithms.

Initially: $\hat{\mathbf{w}}_k(0) = [00\cdots0]$, $\mathbf{w}_k(0) = [00\cdots0]^T$
$A_{km} = 1, \forall K$
for $n = 1$: No.of iterations **do**
  $\mathbf{w}_k(n) = \sum_{m\in K} A_{km}\hat{\mathbf{w}}_m(n)$ (centre node location)
  for $k = 1 : K$ **do**
    for $j = 1 : J$ **do**
      $\mathbf{x}(n)$ is the input reference
      $\tilde{y}_k(n) = \mathbf{x}(n)^{\mathrm{T}}\mathbf{w}_k(n)$
      $e_k(n) = d_k(n) - \sum_{j=1}^{J}\mathbf{S}_{kj}(n) * [\mathbf{x}(n)^{\mathrm{T}}\mathbf{w}_k(n)]$.
      $\hat{\mathbf{w}}_k(n+1) = \mathbf{w}_k(n) - \mu\frac{\partial \mathrm{SCF}}{\partial \mathbf{w}_k(n)}$
      SDF-xSA: $\hat{\mathbf{w}}_k(n+1) =$
      $\mathbf{w}_k(n) +$
      $\mu sign(e_k(n))\frac{[1+\{1-\beta|e_k(n)|\}\exp(-\beta|e_k(n)|)]}{[1+\exp(-\beta|e_k(n)|)]^2}\mathbf{x}'(n)$
      SDF-xLMS: $\hat{\mathbf{w}}_k(n+1) =$
      $\mathbf{w}_k(n) + 2\mu e_k(n)\frac{[1+\{1-\beta e_k^2(n)\}\exp(-\beta e_k^2(n))]}{[1+\exp(-\beta e_k^2(n))]^2}\mathbf{x}'(n)$
      SDF-xSGM: $\hat{\mathbf{w}}_k(n+1) =$
      $\mathbf{w}_k(n) + \mu\frac{2e_k(n)c_1^2[1+(\exp(-\beta\phi)(1-\beta\phi)]\mathbf{x}'(n)}{(e_k^2(n)+c_1^2)^2\left[1+\exp\left(\frac{e_k^2(n)}{e_k^2(n)+c_1^2}\right)(1+exp(-\beta\phi))\right]}$
      SDF-xSW: $\hat{\mathbf{w}}_k(n+1) =$
      $\mathbf{w}_k(n) + \mu\frac{2e_k(n)(|e_k(n)|-1)\delta}{c_2^2(1+|e_k(n)|)^3}[\frac{1+\exp(-\beta\delta)\{1-\beta\delta\}}{\{1+\exp(-\beta\delta)\}^2}]\mathbf{x}'(n)$
      where $\mathbf{x}'(n) = \sum_{j=1}^{J}\mathbf{S}_{kj}(n) * \mathbf{x}(n)^{\mathrm{T}}$
    end for
  end for
end for

characteristics of the noise generated by turbulent environments and dynamic systems can be synthetically obtained by using the equation $x(n+1) = \lambda x(n)[1 - x(n)]$ [13]. The values of $x(0)$ and λ are taken as 0.9 and 4 respectively. In these simulations, impulsive noise is produced by SαS model [43] and Bernoulli Process. The impulsive noise equation is represented by $\Phi(t) = \exp(-|t|^{\alpha})$, where $\alpha(0 < \alpha < 2)$ is called the exponent which decides the heaviness of the distribution. The impulsive noise generated through Bernoulli process is expressed as $v(n) = [1 - \varrho(n)]Y(n) + \varrho(n)Z(n)$, where $\varrho(n)$ is a binary process with probability, $\Pr\{\varrho(n) = 1\} = p_r$ and $\Pr\{\varrho(n) = 0\} = 1 - p_r$, with $0 < p_r < 1$. Moreover, the sequences $Y(n)$ and $Z(n)$ represent two mutually independent noise sequence with the constraint that $Z(n)$ is having larger variance than $Y(n)$. The efficacy of the suggested SD approaches are calculated in terms of the averaged noise reduction (ANR) [43]. The averaged noise reduction is given as

$$\mathrm{ANR}(n) = 20\log\left\{\frac{A_e(n)}{A_d(n)}\right\} \tag{22}$$

where, $A_d(n)$ and $A_e(n)$ are recursive estimation of $d(n)$ and $e(n)$. $A_d(n)$ and $A_e(n)$ are evaluated as $A_d(n) = \eta A_d(n-1) + (1-\eta)|d(n)|$ and $A_e(n) = \eta A_e(n-1) + (1-\eta)|e(n)|$, where η is forgetting factor which is equal to 0.999. The primary and secondary pathways used for the proposed algorithm are from [13]. There are total of five primary paths considered, one corresponding to each of the node. Due to the prevalent acoustic coupling between the error microphone of one node to the loudspeaker of the adjacent nodes, there are five secondary path transfer functions pertaining to each node and total twenty five secondary path transfer functions in the entire set-up of five nodes of the distributed network [13]. The simulations for all the cases are performed with 20 independent trails and 10000 number of iterations.

TABLE 3. Simulation Parameter and ANR Values for Uniformly Distributed Input Reference Noise Using SαS and Bernoulli Impulsive Noise

S.no	Algorithm	Impulsive noise	Parameters		ANR Values in dB				
			μ	L	Node1	Node2	Node3	Node4	Node5
1	SDF-xSA	α = 1.6	2×10^{-8}	7	−15.54	−15.01	−14.47	−14.46	−13.87
		p_r = 0.005	2×10^{-9}	9	−25.29	−24.82	−25.07	−24.81	−24.55
2	SDF-xLMS	α = 1.6	3×10^{-7}	6	−15.56	−15.03	−14.50	−14.48	−13.87
		p_r = 0.005	3×10^{-6}	5	−22.72	−21.97	−22.25	−21.91	−21.49
3	SDF-xSGM	α = 1.6	3×10^{-6}	5	−18.12	−17.59	−17.18	−17.06	−16.44
		p_r = 0.005	3×10^{-6}	5	−33.33	−33.32	−32.53	−31.97	−31.31
4	SDF-xSW	α = 1.6	3×10^{-6}	5	−17.95	−17.42	−16.88	−16.87	−16.25
		p_r = 0.005	3×10^{-6}	5	−33.74	−33.72	−32.89	−32.29	−31.59

μ = learning parameter, L = length of the weight update controller.

The common simulation parameters used in the following all the cases are specified as: $\beta = 10$, $C_1 = 2$, $C_2 = 1$, $\eta = 0.999$, $\lambda = 4$, K = 5, J = 5, $L_s = 4$. The simulation parameters corresponding to each individual cases of different input reference are specified later.

A. UNIFORMLY DISTRIBUTED NOISE

The input reference microphone is subjected to a noise which is uniformly distributed serves as the input reference noise. Table 3 lists the simulation parameters used for all the impulsive noise instances. The ANR curves of the proposed algorithms of SαS model with $\alpha = 1.6$ is depicted in Fig. 5. Fig. 6 represents the ANR values of the suggested techniques with $p_r = 0.005$ of Bernoulli process as impulsive noise integrated at the output. As seen in Figs. 5 and 6, the suggested approach cancels noise equally at all the nodes using the robust nature of the Swish algorithm for SαS and Bernoulli process models of impulsive noise respectively.

B. CHAOTIC NOISE

Two distinct examples are examined in order to determine the efficiency of the suggested technique in various noise interference of SαS and Bernoulli noise model as given in Table 4. The chaotic noise as input is fed to the reference input microphone. Figs. 7 and 8 depict the ANR convergence plots attained at distinct nodes in the distributed scheme for the proposed techniques using various impulsive noise models for chaotic input reference noise. It is

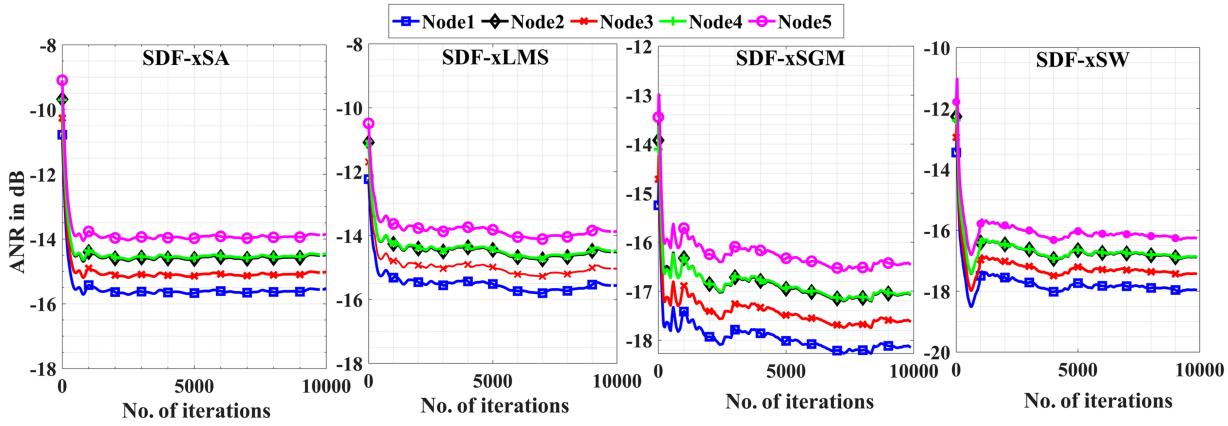

FIGURE 5. Convergence of the suggested SD algorithms for uniformly distributed as input reference using SαS impulsive noise.

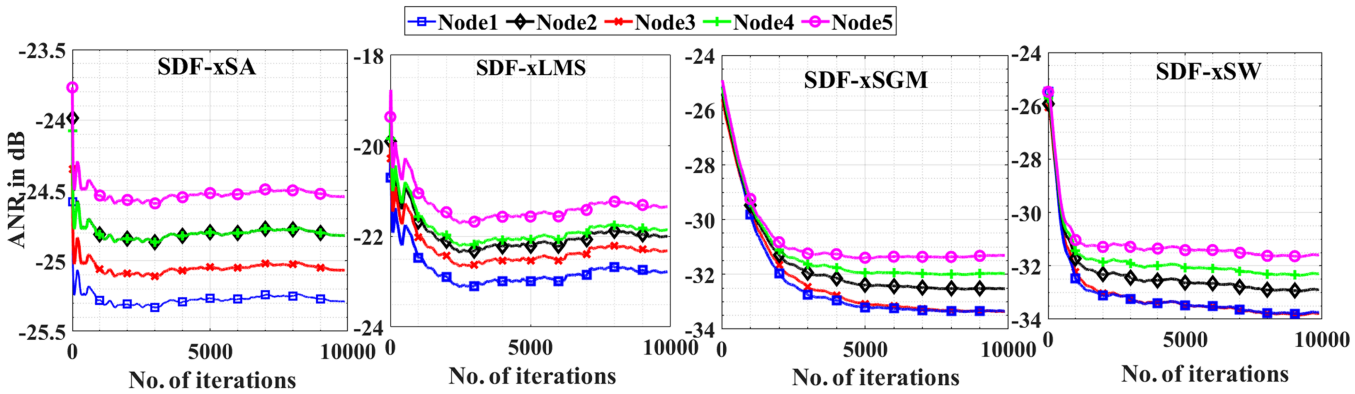

FIGURE 6. Convergence of the suggested SD algorithms for uniformly distributed as input reference using Bernoulli impulsive noise.

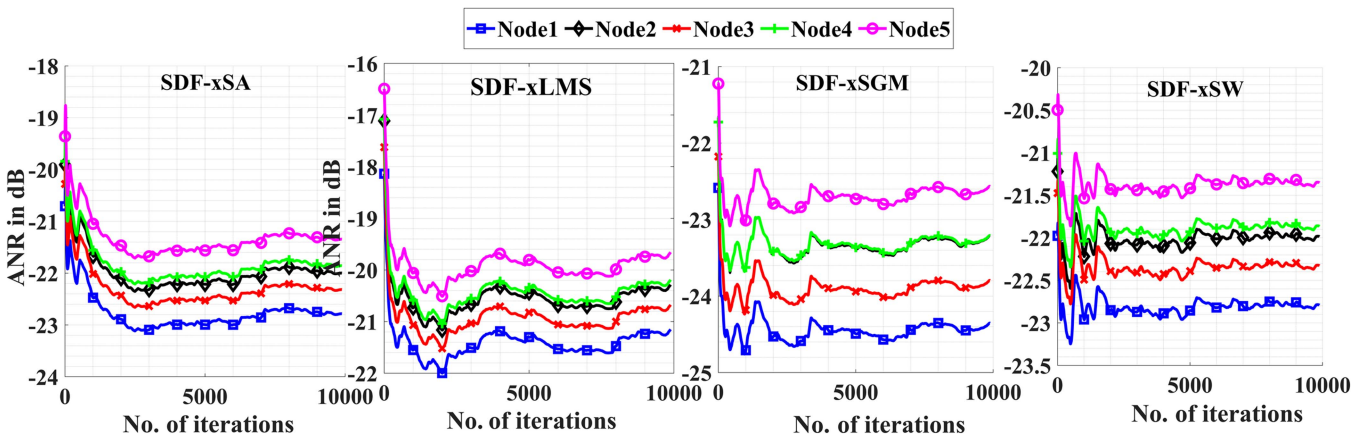

FIGURE 7. Convergence of the suggested SD algorithms for chaotic input reference using SαS impulsive noise.

observed from the ANR plots that the suggested techniques yield significant noise cancellation, maintaining considerable ANR value under impulsive noise environment. This can be attributed to the utilization of Swish based robust cost functions along with the Geman-McClure and Welsh functions.

C. REAL NOISE

Real noise is fed to the input microphone to act as the input reference noise and the impulsive noise is integrated at the output of primary pathways utilizing SαS and Bernoulli process. The three real noise scenarios [44] such as factory noise, airplane cabin and traffic noise are considered as reference

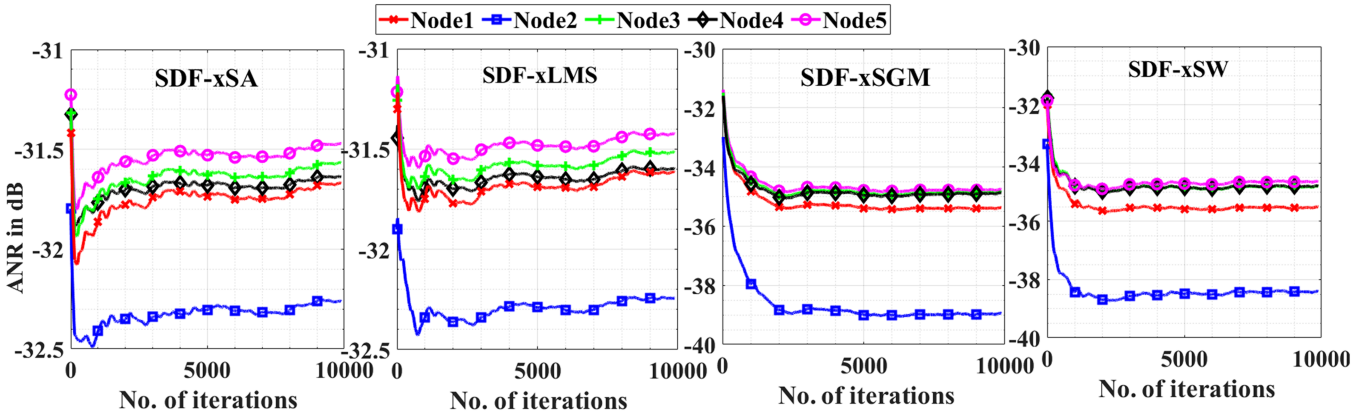

FIGURE 8. Convergence of the suggested SD algorithms for chaotic input reference using Bernoulli impulsive noise.

TABLE 4. Simulation Parameter and ANR Values of Chaotic Input Reference Noise Using SαS and Bernoulli Impulsive Noise

S.no	Algorithm	Impulsive noise	Parameters		ANR Values in dB				
			μ	L	Node1	Node2	Node3	Node4	Node5
1	SDF-xSA	$\alpha = 1.6$	2×10^{-8}	7	−22.78	−21.99	−22.32	−21.86	−21.35
		$p_r = 0.005$	2×10^{-9}	9	−31.63	−32.29	−31.53	−31.62	−31.44
2	SDF-xLMS	$\alpha = 1.6$	3×10^{-7}	6	−21.56	−21.06	−20.67	−20.47	−19.72
		$p_r = 0.005$	3×10^{-6}	5	−31.62	−32.24	−31.52	−31.60	−31.42
3	SDF-xSGM	$\alpha = 1.6$	3×10^{-6}	5	−24.35	−23.21	−23.79	−23.20	−22.58
		$p_r = 0.005$	3×10^{-6}	5	−38.96	−35.40	−34.86	−34.90	−34.76
4	SDF-xSW	$\alpha = 1.6$	3×10^{-6}	5	−22.79	−21.98	−22.34	−21.86	−21.35
		$p_r = 0.005$	3×10^{-6}	5	−35.53	−38.42	−34.81	−34.78	−34.63

μ = learning parameter, L = length of the weight update controller.

TABLE 5. Simulation Parameter and ANR Values for Factory Noise as the Input Reference Using SαS and Bernoulli Impulsive Noise

S.no	Algorithm	Impulsive noise	Parameters		ANR Values in dB				
			μ	L	Node1	Node2	Node3	Node4	Node5
1	SDF-xSA	$\alpha = 1.6$	2×10^{-8}	7	−12.85	−11.78	−12.32	−11.72	−11.17
		$p_r = 0.005$	2×10^{-9}	9	−27.25	−26.69	−26.99	−26.70	−26.35
2	SDF-xLMS	$\alpha = 1.6$	3×10^{-7}	6	−12.59	−11.48	−12.08	−11.50	−10.85
		$p_r = 0.005$	3×10^{-6}	5	−27.17	−26.63	−26.93	−26.64	−26.31
3	SDF-xSGM	$\alpha = 1.6$	3×10^{-6}	5	−14.54	−13.31	−14.02	−13.42	−12.78
		$p_r = 0.005$	3×10^{-6}	5	−30.03	−29.09	−29.60	−29.10	−28.53
4	SDF-xSW	$\alpha = 1.6$	3×10^{-6}	5	−13.16	−11.94	−12.52	−11.94	−11.31
		$p_r = 0.005$	3×10^{-6}	5	−30.24	−29.23	−29.77	−29.24	−28.63

μ = learning parameter, L = length of the weight update controller.

TABLE 6. Simulation Parameter and ANR Values for Airplane Cabin Noise as Input Reference Using SαS Model and Bernoulli Impulsive Noise

S.no	Algorithm	Impulsive noise	Parameters		ANR Values in dB				
			μ	L	Node1	Node2	Node3	Node4	Node5
1	SDF-xSA	$\alpha = 1.6$	2×10^{-8}	7	−13.11	−11.95	−12.58	−11.99	−11.37
		$p_r = 0.005$	2×10^{-9}	9	−25.08	−24.45	−24.79	−24.41	−23.97
2	SDF-xLMS	$\alpha = 1.6$	3×10^{-7}	6	−13.27	−12.11	−12.75	−12.13	−11.52
		$p_r = 0.005$	3×10^{-6}	5	−25.11	−24.46	−24.78	−24.41	−23.99
3	SDF-xSGM	$\alpha = 1.6$	3×10^{-6}	5	−11.94	−10.76	−11.37	−10.79	−10.14
		$p_r = 0.005$	3×10^{-6}	5	−27.54	−26.44	−27.03	−26.47	−25.84
4	SDF-xSW	$\alpha = 1.6$	3×10^{-6}	5	−12.06	−10.92	−11.56	−10.96	−10.32
		$p_r = 0.005$	3×10^{-6}	5	−27.10	−26.08	−26.65	−26.03	−25.47

μ = learning parameter, L = length of the weight update controller.

TABLE 7. Simulation Parameter and ANR Values for Traffic Noise as Input Reference Using SαS Model and Bernoulli Impulsive Noise

S.no	Algorithm	Impulsive noise	Parameters		ANR Values in dB				
			μ	L	Node1	Node2	Node3	Node4	Node5
1	SDF-xSA	$\alpha = 1.6$	2×10^{-8}	7	−14.14	−13.52	−13.68	−13.37	−12.78
		$p_r = 0.005$	2×10^{-9}	9	−35.76	−34.60	−35.22	−34.61	−33.68
2	SDF-xLMS	$\alpha = 1.6$	3×10^{-7}	6	−12.87	−12.14	−12.43	−11.99	11.47
		$p_r = 0.005$	3×10^{-6}	5	−35.73	−34.62	−35.24	−34.65	−34.02
3	SDF-xSGM	$\alpha = 1.6$	3×10^{-6}	5	−16.44	−15.24	−15.88	−15.26	−14.68
		$p_r = 0.005$	3×10^{-6}	5	−36.36	−35.21	−35.82	−35.23	−34.60
4	SDF-xSW	$\alpha = 1.6$	3×10^{-6}	5	−16.41	−15.33	−15.91	−15.34	−14.71
		$p_r = 0.005$	3×10^{-6}	5	−37.11	−35.99	−36.64	−36.04	−35.32

μ = learning parameter, L = length of the weight update controller.

noises. The corresponding simulation parameters and ANR values of factory, airplane cabin and traffic noise are listed in Tables 5–7 respectively.

Fig. 9 illustrates the distinction of ANR values of each node for the factory noise as input using SαS as impulsive noise model. The ANR plots for the suggested methods are shown in Fig. 10 for the Bernoulli process model when the input reference is factory noise. Fig. 11 demonstrates the comparison of ANR values obtained at each of the node for the input reference airplane cabin noise considering SαS model. The ANR plots are shown in Fig. 12 for the different suggested techniques using Bernoulli process model when the input reference is airplane cabin noise. Moreover, four different noise distributions are presented for $Y(n)$ in

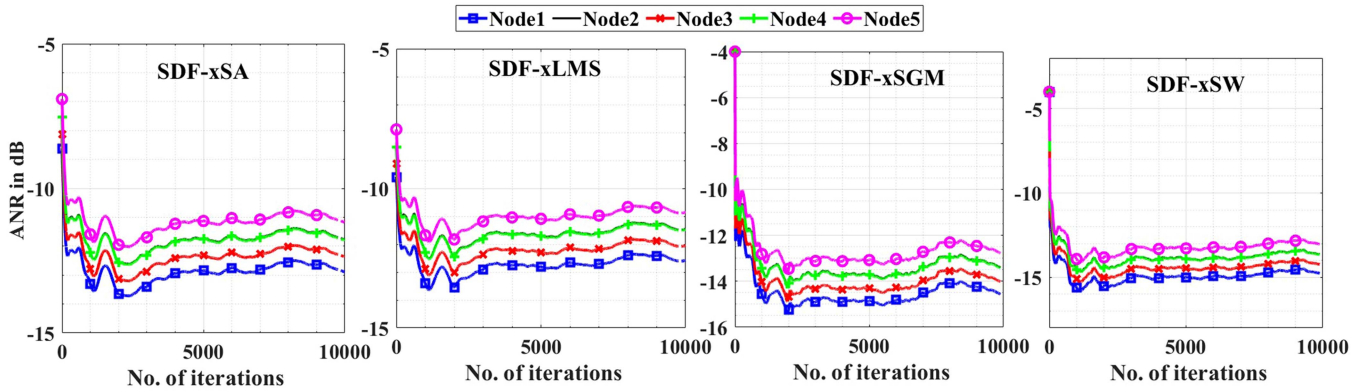

FIGURE 9. Convergence of the suggested SD algorithms for factory noise as input reference using SαS impulsive noise.

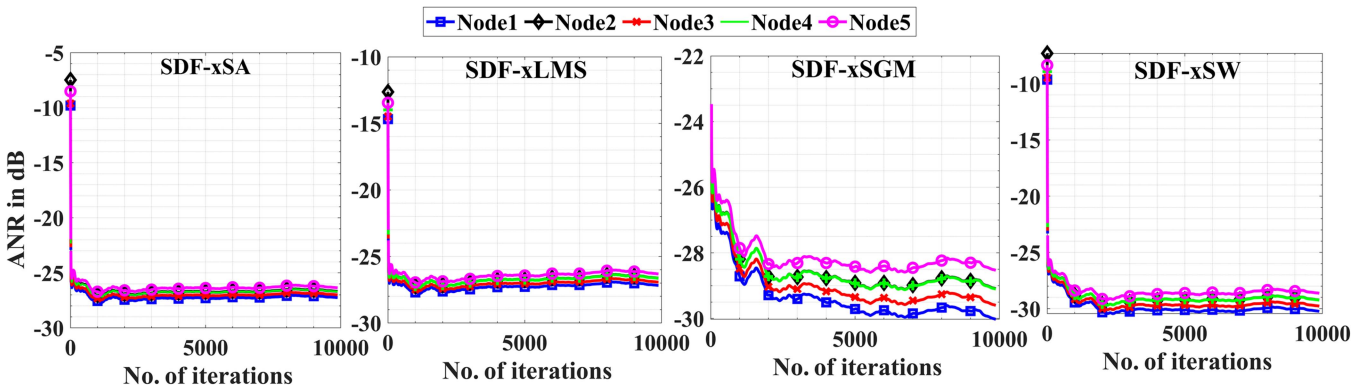

FIGURE 10. Convergence of the suggested SD algorithms for factory noise as input reference using Bernoulli impulsive noise.

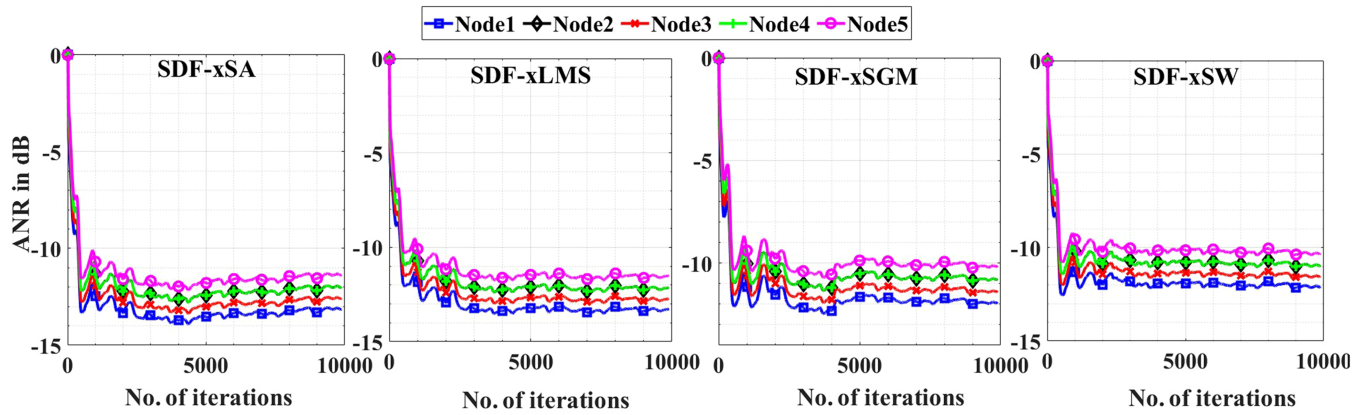

FIGURE 11. Convergence of the suggested SD algorithms for airplane cabin noise as input reference using SαS impulsive noise.

the expression corresponding to generation of impulsive noise as discussed earlier in this section as specified: a) uniformly distributed spanning in the range $[-\sqrt{3}, \sqrt{3}]$ b) Gaussian with zero mean and unity variance c) Laplace characteristic with zero mean and unity variance d) binary spanning the range $[-1, 1]$. This analysis pertaining to various noise distributions are plotted in Fig. 13 corresponding to uniform, Gaussian, Laplace and binary distributions employed for the generation of Bernoulli impulsive noise. It can be inferred from Fig. 13 that the proposed techniques for distributed ANC system offer satisfactory performance in lieu of varied impulsive noise generation through Bernoulli process.

In addition to this, traffic noise is also considered as input to assess the performance of the proposed DANC system while dealing with SαS and Bernoulli based impulsive noise model. Fig. 14 depicts the ANR performance of the proposed Swish family based DANC systems while considering SαS impulsive noise model for different nodes. The comparison of the

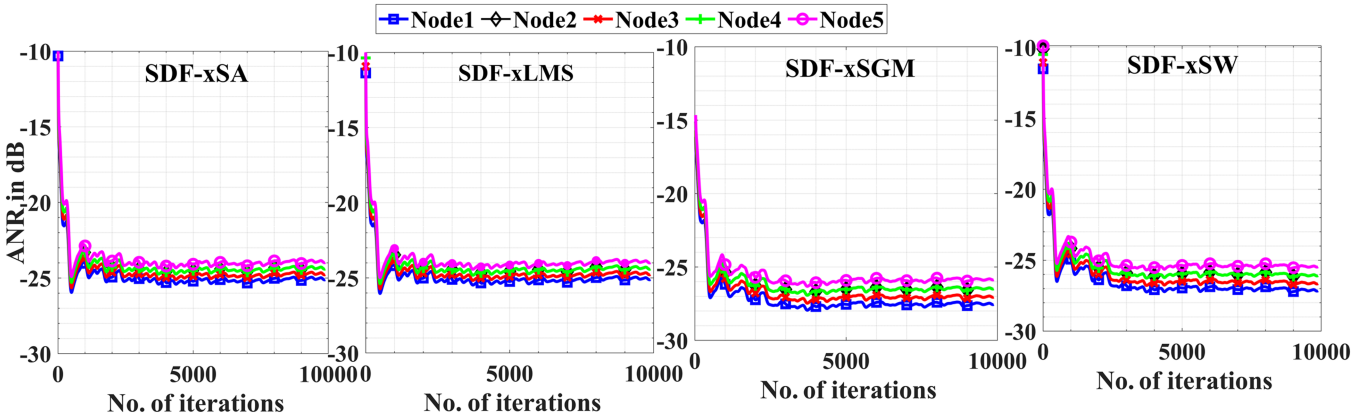

FIGURE 12. Convergence of the suggested SD algorithms for airplane cabin noise as input reference using Bernoulli impulsive noise.

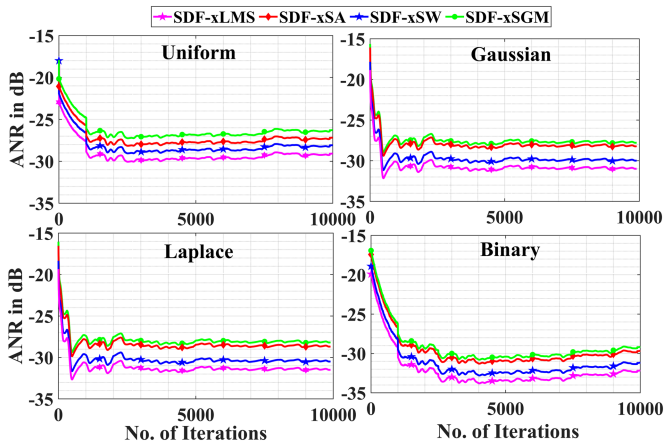

FIGURE 13. Comparison of the proposed Swish based methods for various distributions.

TABLE 8. Simulation Parameter and ANR Values for Three Different $\alpha = 1.3$, 1.6 and 1.8 Values of Impulsive Noise by SαS Model and Uniformly Distributed Noise as the Input Reference

S.no	Algorithm	Impulsive noise	Parameters		ANR Values in dB				
			μ	L	Node1	Node2	Node3	Node4	Node5
1	SDF-xSA	$\alpha = 1.3$	2×10^{-6}	7	−11.37	−11.07	−10.98	−10.57	−9.98
		$\alpha = 1.6$	2×10^{-8}	7	−15.54	−15.01	−14.47	−14.46	−13.87
		$\alpha = 1.8$	2×10^{-9}	8	−18.99	−17.96	−18.48	−17.94	−17.33
2	SDF-xLMS	$\alpha = 1.3$	2×10^{-6}	7	−11.74	−11.43	−11.01	−10.74	−10.06
		$\alpha = 1.6$	2×10^{-7}	6	−15.56	−15.03	−14.50	−14.48	−13.87
		$\alpha = 1.8$	2×10^{-7}	7	−19.22	−18.18	−18.69	−18.17	−17.54
3	SDF-xSGM	$\alpha = 1.3$	2×10^{-7}	7	−13.25	−13.01	−12.45	−12.01	−11.67
		$\alpha = 1.6$	2×10^{-6}	8	−18.12	−17.59	−17.18	−17.06	−16.44
		$\alpha = 1.8$	2×10^{-7}	9	−19.24	−18.22	−18.72	−18.20	−17.57
4	SDF-xSW	$\alpha = 1.3$	2×10^{-7}	7	−12.76	−12.41	−11.57	−11.52	−11.21
		$\alpha = 1.6$	2×10^{-6}	8	−17.95	−17.42	−16.88	−16.87	−16.25
		$\alpha = 1.8$	2×10^{-7}	7	−19.11	−18.06	−18.59	−18.03	−17.44

μ = learning parameter, L = length of the weight update controller.

ANR values while tackling impulsive noise generated through Bernoulli's process is illustrated in Fig. 15 for each node of the distributed ANC system. It can be noted from Figs. 14 and 15 that the proposed Swish based DANC techniques yield sufficient noise reduction performance at each of the nodes of the distributed network. This can be owed to the incorporation of robust Swish strategy along with Softplus and Softsign in Geman-McClure and Welsch functions respectively.

D. COMPARATIVE ANALYSIS OF THE PROPOSED ALGORITHM

The comparative study is made by observing the noise cancellation and convergence of the proposed Swish diffusion filtered-x sign algorithm (SDF-xSA), Swish diffusion filtered-x LMS (SDF-xLMS), Swish diffusion filtered-x Softplus Geman-McClure (SDF-xSGM) and Swish diffusion filtered-x Softsign Welsch (SDF-xSW). It can be seen from Fig. 16, that the suggested Swish diffusion based algorithms result in enhanced noise reduction for distributed ANC setup in comparison with their non Swish counterparts while employing uniformly distributed noise as input.

The impact of variation in the intensity of impulsive noise is studied by plotting the ANR values obtained by all the algorithms while setting $\alpha = 1.3$, 1.6 and 1.8 in SαS noise model referring to heavy, mild and weak impulsiveness. Table 8 lists the simulation parameters and ANR values of the family of proposed method for uniformly distributed as the input with variation in α. Fig. 17 depicts the performance of the system in regard to ANR values incurred at node 5 of various proposed Swish framework dependent algorithm employing uniformly distributed noise as input. As noted from Fig. 17, there is a very marginal improvement in the ANR values pertaining to $\alpha = 1.8$ as compared to $\alpha = 1.6$ and 1.3 respectively. This can be attributed to the condition of weak impulsiveness of the SαS noise model in case of $\alpha = 1.8$ leading to marginal increment in the ANR values. Further, it can be also noted that the suggested Swish based robust DANC algorithms prove their efficacy in maintaining a decent amount of average noise reduction in ANC systems

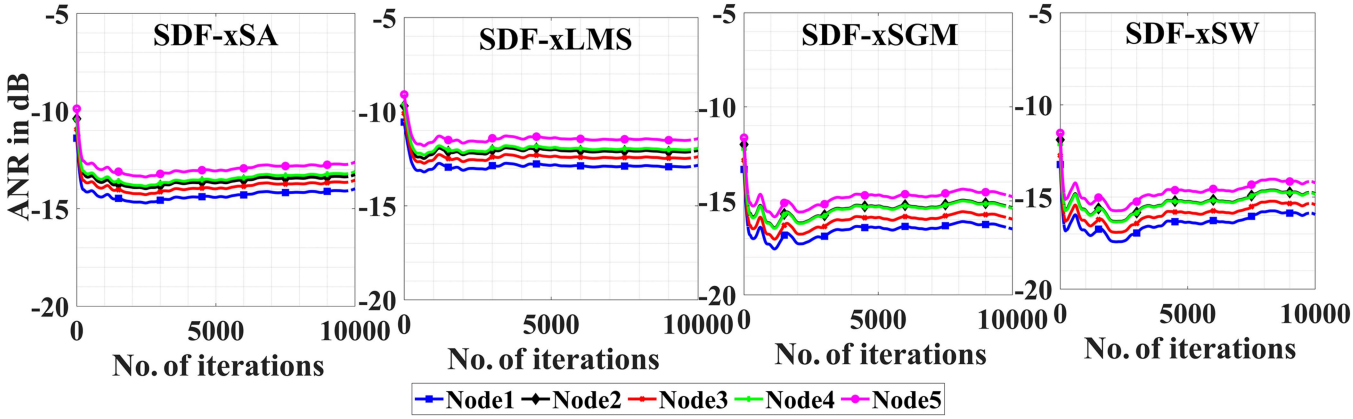

FIGURE 14. Convergence of the suggested SD algorithms for traffic noise as input reference using SαS impulsive noise.

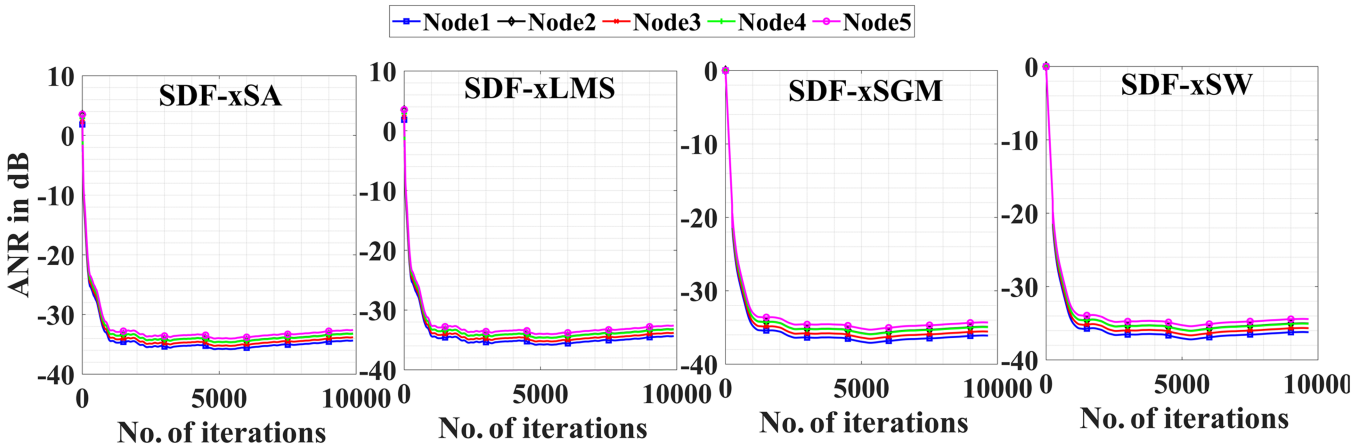

FIGURE 15. Convergence of the suggested SD algorithms for traffic noise as input reference using Bernoulli impulsive noise.

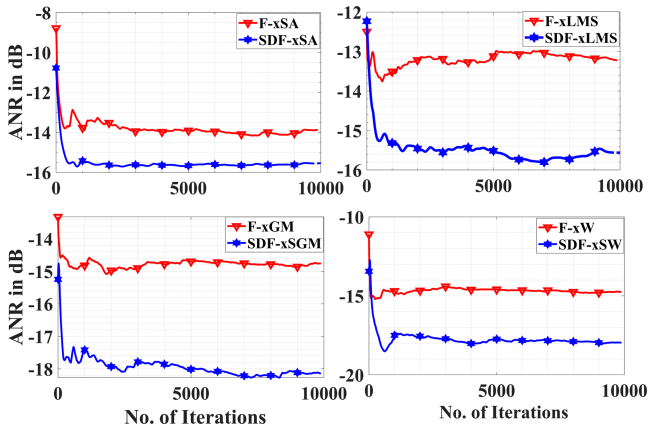

FIGURE 16. Comparison of the suggested techniques (Swish based) with non Swish counterparts.

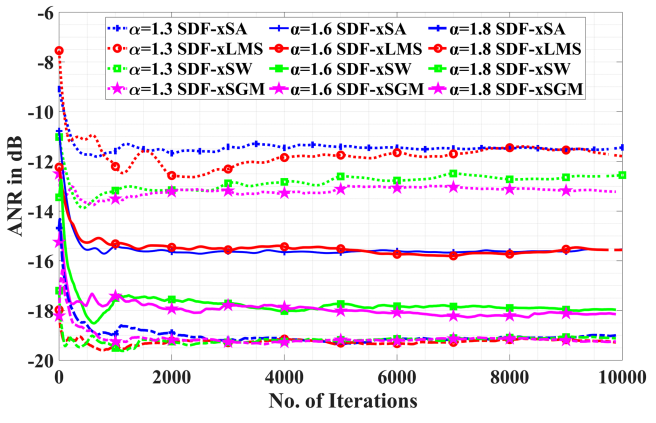

FIGURE 17. Comparison of the suggested techniques with different impulsiveness (α = 1.3,1.6 and 1.8) of SαS model for uniformly distributed input reference.

while handling impulsive noise. In addition, the impact of variation in impulsivity in terms of varying α as 1.3, 1.5 and 1.7 of SαS noise is displayed in Fig. 18 for chaotic noise as input. It represents the comparison of all the proposed robust DANC algorithms constructed on the framework of Swish diffusion along with their non Swish counter part. It can be inferred from Fig. 18 that the proposed Swish family of algorithms are capable of maintaining decent noise

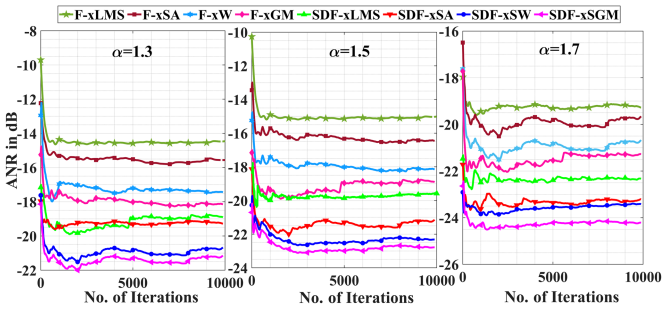

FIGURE 18. Comparison of the proposed techniques for $\alpha = 1.3, 1.5, 1.7$ with non swish counterpart for chaotic input reference.

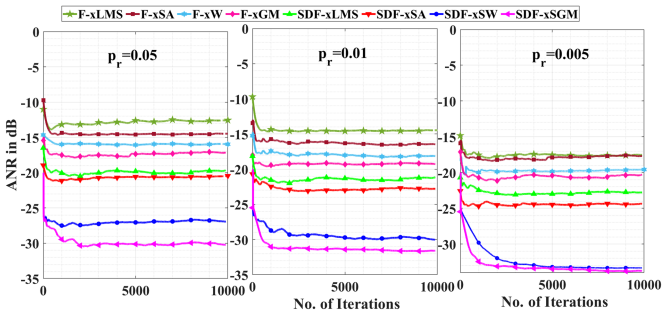

FIGURE 19. Comparison of the proposed techniques for various probability of Bernoulli Gaussian noise with different existing techniques for chaotic input reference.

reduction in the lieu of varying intensity of impulsive noise interference.

In continuation to this, Fig. 19 demonstrates the noise reduction efficacy of the introduced robust algorithms built upon Swish strategy in regard to varying probability ($p_r = 0.05, 0.01, 0.005$) pertaining to impulsive noise generation through Bernoulli process. It can be noted from Fig. 19 that the suggested Swish diffusion based DANC algorithms reveal effective noise reduction in the wake of varying intensity of impulsiveness. The ANR values achieved in view of $p_r = 0.05, 0.01, 0.005$ referring to strong, mild and slightly weak impulsivity of Bernoulli process exhibit worthwhile performance for the distributed ANC system involving Swish based algorithms.

An attempt has been made to assess the performance of the proposed Swish based DANC techniques in comparison to other existing robust methods such as filtered-x LMS (F-xLMS) [7], filtered-x GMCC (F-xGMCC) [27], filtered-x logarithmic hyperbolic cosine adaptive filter (F-xLHCAF) [25], filtered-x Blake Zisserman (F-xBZ) [30], error reused F-xLMS (ErF-xLMS) [32], modified filtered-x robust normalized least mean absolute third (MF-xRNLMAT) [33], modified filtered-x affine-projection-like MCC (MF-xAPLMCC) [34] for uniformly distributed input reference. All the algorithms have been implemented using filtered-x version

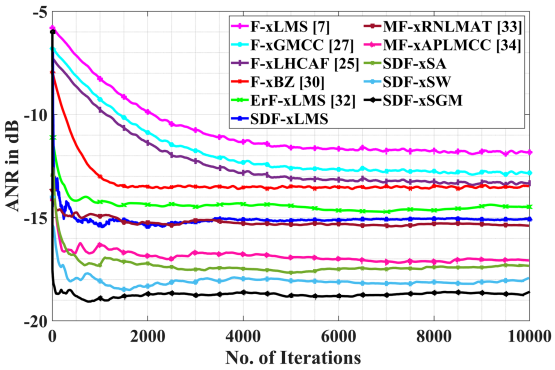

FIGURE 20. Comparison of the proposed DANC techniques with existing techniques for uniformly distributed input reference.

implying the filtering of the reference input signal prior to the weight update process to suit their application to distributed active noise control scenario. It is seen from Fig. 20 that the suggested Swish based class of algorithms outperform the existing robust techniques with impulsive noise $\alpha = 1.6$ in case of SαS impulsive noise model for uniformly distributed noise as input reference. The formulated robust cost functions SGM and SW integrated with Swish diffusion framework utilizing its vanishing gradient property exhibit improved noise mitigation capability in case of impulsive noise interference in a DANC system. The comparative ANR values of the proposed techniques with the existing techniques are listed as: F-xLMS (-11.79 dB), F-xGMCC (-12.83 dB), F-xLHCAF (-13.32 dB), F-xBZ (-13.55 dB), ErF-xLMS (-14.40 dB), SDF-xLMS (-15.04 dB), MF-xRNLMAT (-15.35 dB), MF-xAPLMCC (-17.04 dB), SDF-xSA (-17.41 dB), SDF-xSW (-18.16 dB), SDF-xSGM (-18.62 dB).

Furthermore, tracking capability of the introduced DANC techniques are assessed by varying the primary path characteristics at iteration $n = 5 \times 10^3$. This variation in primary path characteristics are carried out by introducing two samples delay to the original primary path [34]. This is done with the intention to visualize the performance of the robust Swish based DANC techniques involving Softplus and Softsign with Geman-McClure and Welsch algorithms respectively in the situation of sudden changes incurred in the primary path. Fig. 21 shows the tracking performance of the proposed method with the existing techniques employing uniformly distributed noise as input reference with impulsive noise $\alpha = 1.6$ in case of SαS model based impulsive interference. From Fig. 21 it can be observed the proposed method outperforms the existing techniques in case of sudden changes in the primary path. The simulation parameters used for plotting Figs. 20 and 21 are as: F-xLMS ($\mu = 3 \times 10^{-4}$, $L = 10$), F-xGMCC ($\mu = 3 \times 10^{-6}$, $L = 10$, kernel parameter $\Lambda_1 = 2$, shaping parameter $p = 1.7$), F-xLHCAF ($\mu = 3 \times 10^{-5}$, $L = 10$, shaping parameter $\Lambda_2 = 10$), F-xBZ ($\mu = 3 \times 10^{-5}$, $L = 10$, normalization constant $\Gamma = 1$, kernel width $\Lambda_3 = 1$, shaping parameter $\alpha_3 = 2$), ErF-xLMS ($\mu = 3 \times 10^{-4}$, $L =$

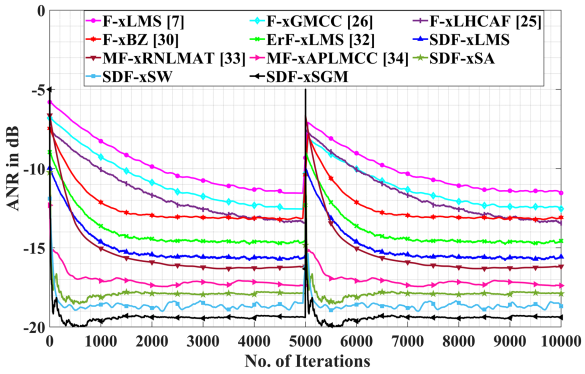

FIGURE 21. Comparison of the tracking performance with change in the primary path.

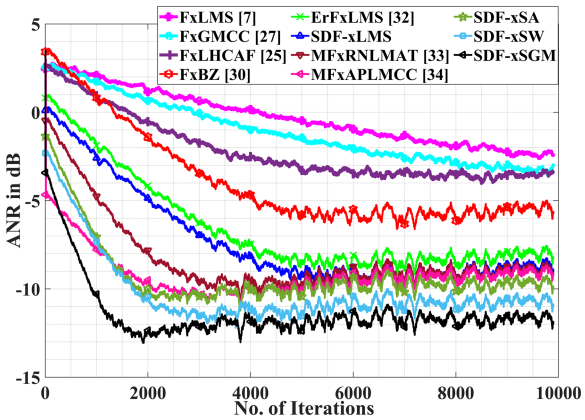

FIGURE 22. Comparison of DANC algorithms for real world scenario.

10), SDF-xLMS ($\mu = 3 \times 10^{-8}$, $L = 6$, shaping parameter $\beta = 10$), MF-xRNLMAT ($\mu = 3 \times 10^{-6}$, $L = 8$, normalization constant $\beta_1 = 1$), MF-xAPLMCC ($\mu = 3 \times 10^{-5}$, $L = 9$, kernel size $\sigma = 8$, projection order $M = 8$), SDF-xSA ($\mu = 2 \times 10^{-8}$, $L = 7$), SDF-xSW ($\mu = 3 \times 10^{-6}$, $L = 5$, shaping parameter $C_2 = 1$), SDF-xSGM ($\mu = 3 \times 10^{-6}$, $L = 5$, shaping parameter $C_1 = 1$).

E. REAL WORLD SCENARIO

In an attempt to verify the robustness of the suggested Swish dependent algorithms in real-world scenario, a database of practical ANC in-ear headphones for acoustic paths have been considered [34]. Fig. 22 plots the ANR curves obtained with the suggested SDF-xSA, SDF-xLMS, SDF-xSGM, and SDF-xSW algorithms as compared to the existing techniques in case of acoustic paths taken from practical ANC in-ear headphone database. As observed from Fig. 22, there is marginal degradation in ANR and convergence of all the proposed and existing algorithms for this practical case.

VI. CONCLUSION

The outliers and burst noises seriously impair the performance of distributed active noise control systems. These disturbances, of impulsive noise with brief duration and residual noise corruption prevent the standard DANC from converging. The proposed SD technique uses the unboundedness and smoothness function as the cost function relying on the parametric value. The findings reveal that the suggested SD methods outperforms existing approaches in terms of ANR improvement and convergence speed. In conclusion, the proposed approach performs better than the existing approaches for distributed active noise control in terms of efficient noise reduction.

REFERENCES

[1] A. Bertrand, "Applications and trends in wireless acoustic sensor networks: A signal processing perspective," in *Proc. 18th IEEE Symp. Commun. Veh. Technol. Benelux*, 2011, pp. 1–6, [Online]. Available: https://api.semanticscholar.org/CorpusID:7867249

[2] M. Ferrer, A. Gonzalez, M. d. Diego, and G. Piñero, "Distributed affine projection algorithm over acoustically coupled sensor networks," *IEEE Trans. Signal Process.*, vol. 65, no. 24, pp. 6423–6434, Dec. 2017, doi: 10.1109/TSP.2017.2742987.

[3] M. Ferrer, M. D. Diego, G. Pinero, and A. Gonzalez, "Active noise control over adaptive distributed networks," *Signal Process.*, vol. 107, pp. 82–95, 2015, doi: 10.1016/j.sigpro.2014.07.026.

[4] E. Bjarnason, "Analysis of the filtered-x LMS algorithm," *IEEE Trans. Speech Audio Process.*, vol. 3, no. 6, pp. 504–514, Nov. 1995, doi: 10.1109/89.482218.

[5] T. Padhi, M. Chandra, and A. Kar, "A new hybrid active noise control system with convex combination of time and frequency domain filtered-X LMS algorithms," *Circuit Syst. Signal Process.*, vol. 38, pp. 3275–3294, 2018, doi: 10.1007/s00034-018-0784-x.

[6] T. Padhi, M. Chandra, and A. Kar, "Performance evaluation of hybrid active noise control systems with online secondary path modelling," *Appl. Acoust.*, vol. 133, pp. 215–236, 2018, doi: 10.1016/j.apacoust.2017.12.029.

[7] F. Yang, J. Guo, and J. Yang, "Stochastic analysis of the filtered-x LMS algorithm for active noise control," *IEEE/ACM Trans. Audio, Speech, Lang. Process.*, vol. 28, pp. 2252–2266, 2020, doi: 10.1109/TASLP.2020.3012056.

[8] J. Zhang, T. D. Abhayapala, W. Zhang, P. N. Samarasinghe, and S. Jiang, "Active noise control over space: A wave domain approach," *IEEE/ACM Trans. Audio, Speech, Lang. Process.*, vol. 26, no. 4, pp. 774–786, Apr. 2018, doi: 10.1109/TASLP.2018.2795756.

[9] J. Zhang, T. D. Abhayapala, P. N. Samarasinghe, W. Zhang, and S. Jiang, "Multichannel active noise control for spatially sparse noise fields," *J. Acoust. Soc. Amer.*, vol. 140, pp. 510–516, 2016, doi: 10.1121/1.4971878.

[10] S. Zhang, L. Zhang, D. Meng, and X. Zhang, "A hybrid feedforward/feedback multi-channel active control system with optimization for cancelling road noise inside a vehicle cabin," *Appl. Acoust.*, vol. 201, 2022, Art. no. 109128, doi: 10.1016/j.apacoust.2022.109128.

[11] D. Shi, B. Lam, X. Shen, and W. S. Gan, "Multichannel two-gradient direction filtered reference least mean square algorithm for output-constrained multichannel active noise control," *Signal Process.*, vol. 207, 2023, Art. no. 108938, doi: 10.1016/j.sigpro.2023.108938.

[12] Y. J. Chu, C. M. Mak, Y. Zhao, S. C. Chan, and M. Wu, "Performance analysis of a diffusion control method for ANC systems and the network design," *J. Sound Vib.*, vol. 475, pp. 22–460, 2020, doi: 10.1016/j.jsv.2020.115273.

[13] R. Kukde, M. S. Manikandan, and G. Panda, "Incremental learning based adaptive filter for nonlinear distributed active noise control system," *IEEE Open J. Signal Process.*, vol. 1, pp. 1–13, 2020, doi: 10.1109/OJSP.2020.2975768.

[14] S. J. Elliott and C. C. Boucher, "Interaction between multiple feedforward active control systems," *IEEE Trans. Speech Audio Process.*, vol. 2, no. 4, pp. 521–530, Oct. 1994, doi: 10.1109/89.326611.

[15] N. V. George and G. Panda, "A particle swarm optimization based decentralized nonlinear active noise control system," *IEEE Trans. Instrum. Meas.*, vol. 61, no. 12, pp. 3378–3386, Dec. 2012, doi: 10.1109/TIM.2012.2205492.

[16] C. G. Lopes and A. H. Sayed, "Diffusion least-mean squares over adaptive networks: Formulation and performance analysis," *IEEE Trans. Signal Process.*, vol. 56, no. 7, pp. 3122–3136, Jul. 2008, doi: 10.1109/TSP.2008.917383.
[17] A. A. Haghrah, M. A. Tinati, and T. Y. Rezaii, "Analysis of incremental LMS adaptive algorithm over wireless sensor networks with delayed-links," *Digit. Signal Process.*, vol. 88, pp. 80–89, 2018, doi: 10.1016/j.dsp.2019.02.006.
[18] E. Masry and F. Bullo, "Convergence analysis of the sign algorithm for adaptive filtering," *IEEE Trans. Inf. Theory*, vol. 41, no. 2, pp. 489–495, Mar. 1995, doi: 10.1109/18.370150.
[19] E. Walach and B. Widrow, "The least mean fourth (LMF) adaptive algorithm and its family," *IEEE Trans. Inf. Theory*, vol. IT-30, no. 2, pp. 275–283, Mar. 1984, doi: 10.1109/TIT.1984.1056886.
[20] Vasundhara, "Re-weighted zero attracting adaptive exponential FLAF with maximum correntropy criterion for robust sparse nonlinear system identification," *Digit. Signal Process.*, vol. 130, 2022, Art. no. 103664, doi: 10.1016/j.dsp.2022.103664.
[21] Vasundhara, "Sparsity aware affine-projection-like filtering integrated with robust set membership and M-estimate approach for acoustic feedback cancellation in hearing aids," *Appl. Acoust.*, vol. 175, 2021, Art. no. 107778, doi: 10.1016/j.apacoust.2020.107778.
[22] Vasundhara, "Robust filtering employing bias compensated M-estimate affine-projection-like algorithm," *Electron. Lett.*, vol. 56, pp. 241–243, 2020, doi: 10.1049/el.2019.2763.
[23] L. R. Vega, H. Rey, J. Benesty, and S. Tressens, "A new robust variable step-Size NLMS Algorithm," *IEEE Trans. Signal Process.*, vol. 56, no. 5, pp. 1878–1893, May 2008, doi: 10.1109/TSP.2007.913142.
[24] K. Kumar, R. Pandey, S. S. Bhattacharjee, and N. V. George, "Exponential hyperbolic cosine robust adaptive filters for audio signal processing," *IEEE Signal Process. Lett.*, vol. 28, pp. 1410–1414, 2021, doi: 10.1109/LSP.2021.3093862.
[25] B. P. Mishra, T. Panigrahi, A. M. Wilson, and S. L. Sabat, "A robust diffusion algorithm using logarithmic hyperbolic cosine cost function for channel estimation in wireless sensor network under impulsive noise environment," *Digit. Signal Process.*, vol. 23, 2022, Art. no. 103384, doi: 10.1016/j.dsp.2022.103384.
[26] N. C. Kurian, K. Patel, and N. V. George, "Robust active noise control: An information theoretic learning approach," *Appl. Acoust.*, vol. 117, pp. 180–184, 2017, doi: 10.1016/j.apacoust.2016.10.026.
[27] Y. Zhu and H. Zhao, "A robust generalized maximum correntropy criterion algorithm for active noise control," *IFAC-PapersOnLine*, vol. 52, pp. 299–303, 2019, doi: 10.1016/j.ifacol.2019.12.425.
[28] Y. Zhu, H. Zhao, X. Zeng, and B. Chen, "Robust generalized maximum correntropy criterion algorithms for active noise control," *IEEE/ACM Trans. Audio, Speech, Lang. Process.*, vol. 28, pp. 1282–1292, 2020, doi: 10.1109/TASLP.2020.2982030.
[29] N. V. George and G. Panda, "A robust evolutionary feedforward active noise control system using Wilcoxon norm and particle swarm optimization algorithm," *Expert Syst. With Appl.*, vol. 39, pp. 7574–7580, 2012, doi: 10.1016/j.eswa.2012.01.038.
[30] K. Kumar, M. L. N. S. Karthik, and N. V. George, "Generalized modified Blake–Zisserman robust sparse adaptive filters," *IEEE Trans. Syst., Man, Cybern.: Syst.*, vol. 53, no. 1, pp. 647–652, Jan. 2023, doi: 10.1109/TSMC.2022.3184073.
[31] M. Ferrer, M. D. Diego, G. Pinero, and A. Gonzalez, "Affine projection algorithm over acoustic sensor networks for active noise control," *IEEE/ACM Trans. Audio, Speech, Lang. Process.*, vol. 29, pp. 448–461, 2021, doi: 10.1109/TASLP.2020.3042590.
[32] Q. Zhang, D. Lin, Y. Xiao, Y. Zheng, and S. Wang, "Error reused filtered-X least mean square algorithm for active noise control," *IEEE/ACM Trans. Audio, Speech, Lang. Process.*, vol. 32, pp. 397–412, 2024, doi: 10.1109/TASLP.2023.3330077.
[33] A. Mirza, F. Afzal, A. Zeb, A. Wakeel, W. S. Qureshi, and A. Akgul, "New FxLMAT-based algorithms for active control of impulsive noise," *IEEE Access*, vol. 11, pp. 81279–81288, 2023, doi: 10.1109/ACCESS.2023.3293647.
[34] Y. R. Chien, C. H. Yu, and H. W. Tsao, "Affine projection like maximum correntropy criteria algorithm for robust active noise control," *IEEE/ACM Trans. Audio, Speech, Lang. Process.*, vol. 30, pp. 2255–2266, 2022, doi: 10.1109/TASLP.2022.3190720.
[35] M. Jiang, Y. Gao, Z. Cai, J. Xu, and S. Ou, "Combined regularization factor for affine projection algorithm using variable mixing factor," *IEEE Access*, vol. 10, pp. 120630–120639, 2022, doi: 10.1109/ACCESS.2022.3222335.
[36] K. Kumar, R. Pandey, S. S. Bora, and N. V. George, "A robust family of algorithms for adaptive filtering based on the arctangent framework," *IEEE Trans. Circuits Syst. II: Exp. Briefs*, vol. 69, no. 3, pp. 1967–1971, Mar. 2022, doi: 10.1109/TCSII.2021.3129536.
[37] R. Kukde, M. S. Manikandan, and G. Panda, "Robust distributed active noise control in presence of secondary path and error sensor disturbances," in *Proc. IEEE Region 10 Conf.*, 2017, pp. 369–374, doi: 10.1109/TENCON.2017.8227892.
[38] T. Li, S. Lian, S. Zhao, J. Lu, and I. S. Burnett, "Distributed active noise control based on an augmented diffusion FxLMS algorithm," *IEEE/ACM Trans. Audio, Speech, Lang. Process.*, vol. 31, pp. 1449–1463, 2023, doi: 10.1109/TASLP.2023.3261742.
[39] C. Jing and Y. Jun, "A distributed FxLMS algorithm for narrowband active noise control and its convergence analysis," *J. Sound Vib.*, vol. 532, 2022, Art. no. 116986, doi: 10.1016/j.jsv.2022.116986.
[40] F. Miguel et al., "Assessment of stability of distributed FxLMS active noise control systems," *Signal Process.*, vol. 210, 2023, Art. no. 109087, doi: 10.1016/j.sigpro.2023.109087.
[41] F. Huang, J. Zhang, and S. Zhang, "A family of robust adaptive filtering algorithms based on sigmoid cost," *Signal Process.*, vol. 149, pp. 179–192, 2018, doi: 10.1016/j.sigpro.2018.03.013.
[42] P. Ramachandran, B. Zoph, and Q. Le, "Swish: A self-gated activation function," 2017, *arXiv.1710.05941*.
[43] R. Kranthi and Vasundhara, "A robust adaptive filter for diffusion strategy-based distributed active noise control," *IETE J. Res.*, pp. 1–15, 2023, doi: 10.1080/03772063.2023.2222099.
[44] F. Font, G. Roma, and X. Serra, "Freesound technical demo," in *Proc. 21st ACM Int. Conf. Multimedia, Assoc. Comput. Mach.*, 2013, pp. 411–412, doi: 10.1145/2502081.2502245.

RAJAPANTULA KRANTHI (Graduate Student Member, IEEE) received the B.Tech. degree in electronics and communication engineering from Jawaharlal Nehru Technological University, Hyderabad, Hyderabad, India, in 2008, and the M.Tech. degree in digital electronics and communication systems from Jawaharlal Nehru Technological University, Kakinada, Kakinada, India, in 2011. She is currently working toward the Ph.D. degree in electronics and communication engineering with National Institute of Technology, Warangal, Hanamkonda, India. Her primary research interests include signal processing for dispersed networks and adaptive signal processing.

VASUNDHARA (Member, IEEE) received the graduation degree in electronics and telecommunications from the National Institute of Technology, Raipur, Raipur, India, the postgraduation degree in microelectronics and VLSI from the National Institute of Technology Durgapur, Durgapur, India, and the Ph.D. degree from Indian Institute of Technology Bhubaneswar, Bhubaneswar, India. She is currently an Assistant Professor with the Department of Electronics and Communication Engineering, National Institute of Technology Warangal, Hanamkonda, India. She was an Assistant Professor with the Indian Institute of Information Technology, Design and Manufacturing, Kancheepuram, Chennai, India. Dr. Vasundhara has numerous publications in prestigious journals such as IEEE TRANSACTIONS ON CIRCUITS AND SYSTEMS, *Elsevier Digital Signal Processing*, *IET Electronics Letters*, and others. Her research interests include adaptive signal processing, distributed systems, system identification and parameter estimation and applications in health care systems.

ASUTOSH KAR (Senior Member, IEEE) has been a Faculty Fellow with the Indian Institute of Technology –Madras, Chennai, India, since 2021 and an Associate Professor with the Department of ECE, Dr. B. R. Ambedkar National Institute of Technology Jalandhar, Jalandhar, India, since 2023. He was an Assistant Professor (Grade-I) with the Indian Institute of Information Technology, Design and Manufacturing, Kancheepuram, Chennai, India, for 4.8 years and with the Birla Institute of Technology and Science, Pilani, Pilani, India for close to 2 years. He is also a Visiting Research Scientist with the ESAT Lab, Dept. of Electrical Engineering, Katholic University of Leuven, Belgium, King Mongkut's Institute of Technology Ladkrabang, Bangkok, Thailand, University of Kragujevac Serbia, Kragujevac, Serbia, and the Department of Medical Physics and Acoustics, University of Oldenburg, Oldenburg, Germany. He has more than 100 research papers in reputed journals and conferences at the international level. His research interests include signal processing, adaptive filters, machine learning, acoustics and audio signal analysis, and hearing-aid system designs. He was the recipient of the Marie-Curie Postdoctoral fellowship from the Department of Electronic Systems, Aalborg University, Denmark from 2015 to 2017 for a period of 16 months. Dr. Kar has implemented several industry-sponsored projects for Samsung Electronics, Ventech Solutions USA, Titan R D, and Oretes Consulting respectively. He is currently working on the India-Korea bilateral project and India-Serbia bilateral, sponsored by the DST. He is an Associate Editor for *Circuit Systems and Signal Processing*, Springer.

MADS GRÆSBØLL CHRISTENSEN (Senior Member, IEEE) received the M.Sc., Ph.D., and Dr.Techn. degrees from Aalborg University, Aalborg, Denmark, in 2002, 2005, and 2022. He is currently the Head of Department and Full Professor with the Department of Electronic Systems, Aalborg University. He was formerly with the Department of Architecture, Design and Media Technology, AAU and has been held visiting positions with Philips Research Labs, ENST, UCSB, and Columbia University, New York, NY, USA. He has authored or coauthored four books and about 300 papers in peer-reviewed conference proceedings and journals, and he has given multiple tutorials and keynote talks at major international conferences. His research interests include audio and acoustic signal processing where he has worked on topics such as microphone arrays, noise reduction, signal modeling, speech analysis, audio classification, and audio coding. Dr. Christensen was the recipient of several awards, including best paper awards, the Spar Nord Foundation's Research Prize, a Danish Independent Research Council Young Researcher's Award, Statoil Prize, EURASIP Early Career Award, and an IEEE SPS best paper award. He is a beneficiary of major grants from the Independent Research Fund Denmark, the Villum Foundation, and Innovation Fund Denmark. He is currently an Editor-in-Chief of *EURASIP Journal on Audio, Speech, and Music Processing* and is Chairman of EURASIP Technical Area Committee in Acoustic, Speech and Music Signal Processing. He is a former Senior Area Editor of IEEE SIGNAL PROCESSING LETTERS, Associate Editor for IEEE/ACM TRANSACTIONS ON AUDIO, SPEECH, AND LANGUAGE PROCESSING, Associate Editor for IEEE SIGNAL PROCESSING LETTERS, and Member of the IEEE Audio and Acoustic Signal Processing Technical Committee. He is a Member of EURASIP, and Fellow of the Danish Academy of Technical Sciences.